International Journal for Multidisciplinary Research (IJFMR)
E-ISSN: 2582-2160 ● Website: www.ijfmr.com ● Email: editor@ijfmr.com

Comparative Analysis of Solar Chimney Power Plant Chimney Design: Performance Evaluation and Material Cost Comparison

Samiran Ghorai[1], Ramesh Chandra Borah[2], Tanmoy Choudhury[3]

[1,2]The Assam Kaziranga University, Jorhat,785006, India.
[3]Defence Research and Development Organization, Hyderabad, 500059, India.

Abstract:
This paper investigates different configurations of solar chimney design in a solar chimney power plant system. Mathematical analysis of the system has been done in Ansys software. The results of the maximum (inlet) velocity, pressure, efficiency, and temperature of the air are obtained for base type, convergent, divergent, sudden contraction, and sudden expansion types of chimneys. Furthermore, the electrical power output of Solar Chimney Power Plants has been determined for different chimney types. In this analysis, one Solar Chimney Power Plant (SCPP) with a solar collector diameter of 258 m and a chimney height of 197 meters and outlet diameter of 10 m has been taken as the basis. It has been found that sudden expansion and divergent types of chimneys give higher output power than the other types of chimneys. Also, while calculating the cost of materials of the different types of chimneys, it has been found that the sudden expansion type of chimneys is costing less than other types of chimneys. When power output was compared, it was found that the sudden expansion type of chimney gives higher output than other chimneys. Detailed simulation, testing, and analysis are necessary to consolidate the results.

Keywords: Solar chimney power Plant, design, different types of chimneys, performance analysis, cost.

1. INTRODUCTION:

The emission of greenhouse gases from the combustion of fossil fuels is a well-known global problem. To reduce the emission of greenhouse gases whole world is turning towards renewable energy. Continuous growth in population and globalization are affecting in increasing demand for power causing fast decreases in natural resources and thus shifting focus towards renewable sources of energy. Weather condition change has become a burning topic in every part of the world, and researchers are finding ways to use different energy sources to cope with the deteriorating environmental condition. Solar energy, one of the prime sources of renewable energies, has gained big popularity in the last period of ten years. Solar Chimney Power Plant (SCPP) technology is one of these. In its easiest form, SCPP consists of a transparent solar collector, which heats the air inside it because of the greenhouse effect, hot air moves up through a chimney due to natural draught produced by the density difference of hot and cold air. The hot air finally releases into the atmosphere. The draught produces a suitable pressure difference between the chimney base and the collector entrance. A wind turbine is placed at the base of the chimney which converts the kinetic energy to mechanical work, which further generates electricity. SCPP is providing clean energy causing zero pollution and generating a suitable amount of power. Solar radiation, collector area, chimney

height, and chimney type are the main factor for the efficiency and performance of the power plant. The solar chimney design is a challenge to keep the vortex flow of air low to ensure smooth flow through the chimney. The chimney height is a crucial parameter to contribute to the variation of air velocity. The design and Performance study is done by controlling the chimney configuration. Development and simulation of SCPP with an optimum height of the chimney, the material used, and the selected method of fabrication (the process that is used to shape, cut, or mold materials into items) will be the deciding factors in creating more advancement in the field of green energy for sustainable development.

In 1903, Cabanyes first proposed the concept of the SCPP and then the Solar Chimney Power Plant (SCPP) system was proposed in the late 1970s by professor J. Schlaich and tested with a prototype model in Manzanares, Spain in the early 1980s [1,2]. This Spanish prototype has a chimney of height 194.6m, and chimney radius is 5.08 m, a collector radius is 122 m, and an average height of the collector roof is 1.85 m, which was able to generate actual power output of 37 kw. The solar radiation intensity was 850 w/m^2.It used to be in operation for an average of 9hrs per day. The maximum solar intensity is available only from 2 to 4hrs. There are inherent disadvantages of a tall chimney and environmental hazards, also the manufacturing cost is high for a tall chimney. This plant was operated automatically for approximately 7 years, which demonstrated the feasible operation of the SCPP. In recent times Computational Fluid Dynamics (CFD) solutions considering 2D and 3D models have been incorporated to validate and optimize the performance of SCPP. Pasumarthi and Sherif [3,4] developed a mathematical model to study the effects of various environmental conditions and geometry on the flow and heat transfer characteristics and output power of the solar chimney, and they compared it with their experimental data and reported that overall results were encouraging. In their experimental model area of collector base has been increased and also put some absorber material in the collector base which has increased the output. Lodhi [5] presented a comprehensive analysis of the chimney design, power production, and efficiency, and estimated the cost of the SCPP setup in developing nations. Bernardes et al. [6] presented a theoretical analysis of a solar chimney, operating on natural laminar convection under a steady state. Gannon and Backstrom [7,8] presented an air standard cycle analysis of the SCPP for the calculation of limiting performance efficiency, and the relationship between the main variables including chimney friction, turbine system, and exit kinetic energy losses. Gannon and Backstrom [9] also presented an experimental investigation of the performances of a solar chimney turbine. The measured results showed that the solar chimney turbine presented has a total-to-total efficiency (ratio of actual work output of the turbine to the net input energy supplied in the form of hot air) of 85% - 90% and total to-static efficiency (used as a basis to obtain expressions for the optimum outlet blade angle and for the axial interference factor of a Horizontal Axis Wind Turbine or HAWT turbine blade ring) of 77% - 80% over the design range. Later, Gannon and Backstrom [10] presented an analytical equation in terms of turbine flow and load coefficient, and degree of reaction, to express the influence of each coefficient on turbine efficiency. Pastohr et al. [11] carried out a two-dimensional steady-state numerical simulation study on the whole SCPP system which consists of the energy storage layer, solar collector, turbine, and chimney obtained the distribution of velocity, pressure, and temperature inside the collector. Schlaich et al. [12] made an analysis of the operation principle of an SCPP system and predicted the commercial application prospects of large-scale SCPP systems. Pretorius and Kroger [13] evaluated the influence of a developed convective heat transfer equation, a more accurate turbine inlet loss coefficient, and the quality of collector roof glass. Bilgen and Rheault [14] designed an SCPP system for power production at high latitudes and evaluated its performance.The results showed that solar chimney power plants at high latitudes may have satisfactory

thermal performance and produce as much as 85% of the same plants in southern locations with horizontal collector field. The overall thermal performance of these plants is a little less than 0.5%.Koonsrisuk and Chitsomboon [15] proposed dimensionless variables to guide the experimental study of flow in a small-scale solar chimney and employed a CFD methodology to explore the results. Chimney configuration is an important parameter in respect of power generation. Cuce et al. [16] and Siyang Hu et al. [17] have investigated the influence of area ratio on the performance of SCPP through a justified 3D axis, CFD Model. They have taken the geometric characteristics of the Manzanares pilot plant in their numerical model. The area ratio is varied from 0.5 to 10 to cover both convergent and divergent solar chimney designs. They have indicated that it is possible to improve the generation power from 54.3 KW to 168.5 KW with an optimal area ratio value. They have also concluded that the streamline in the chimney is disturbed when the divergence angle is increased up to 2.5 degrees. Das Pritam and V.P. Chandramohan [18] has also done a theoretical study on the performance of SCPP employing divergent chimney and found the optimal divergence angle to be equal to 2 degrees which gives enhanced performances. Koonsrisuk and Chitsomboon [19] have concluded from the theoretical study of SCPP employing CFD technology that proper combination between the sloping collector roof and divergent top chimney can produce power as much as 100 times that of a conventional solar chimney power plant. Abdallah Bouabidi et al. [20] have studied the effect of chimney configuration on the local flow characteristics of SCPP. They have studied experimentally taking standard chimneys, divergent, convergent, and opposing chimneys. They have concluded that maximum velocity emerges with divergent configurations. Singh et al. [21] have investigated a novel design of chimney and concluded that suitable design changes in collector, chimney. Integrating an efficient bell-mouth at the inlet can substantially increase the air velocity by about 270% and hence drastically enhance the turbine power output compared to conventional design. So, it is necessary to explore different types of design of chimneys and find out an optimum design of the chimney. Divergent, sudden contraction and sudden expansion types of chimneys are universally better than basic chimneys and convergent chimneys. The choice of chimney design depends on various factors such as the specific application, flow conditions, and desired performance outcomes. Each type of chimney has its advantages and disadvantages, and their effectiveness depends on the context in which they are used. So, in this paper design and performance analysis of different types of chimneys has been done. Studying different types of chimneys for a solar chimney power plant is essential for optimizing efficiency, ensuring safety, minimizing environmental impact, and making informed decisions that contribute to the successful implementation and operation of the power plant.

Nomenclature:

A_{ch}	Chimney area, m^2
C_p	Specific heat of air, kJ/kg K
D_{ch}	Chimney outlet dia, m
D_{coll}	Collector dia, m
H_{ch}	Chimney height, m
g	Acceleration due to gravity, m/s^2
G	Amount of solar intensity radiation absorbed, W/m^2
I_s	Solar insolation on collector, W/m^2
r	Radius of the absorber plate, m
T_a	Ambient temperature, K
η_t	Turbine efficiency

η_{coll}	Collector efficiency
V_{ch}	Velocity through the chimney, m/s
ρ_{air}	Ambient air Density, kg/m^3
W_{ch}	Flow Power at bottom of the chimney, W
W_e	Electric power produced by the generator, W
W_t	Mechanical power (Maximum) developed by the wind turbine, W
η_{ch}	Chimney efficiency
T_h	Hot air temperature, K
T_0	Collector outlet temperature, K
ΔT	Temperature difference between hot air and ambient air temperature, K
τ	Transmissivity of the cover
F_R	Heat removal factor
A_{coll}	Area of the collector, m^2
U_L	Overall heat transfer coefficient, W/m^{2}K

2. OBJECTIVE:

In this paper, a systematic study of all related key parameters influencing the performance of SCPP has been carried out in subsequent sections with summarizing tables. The main objective is to study power output, temperature rise, Collector Base (CB) maximum velocity, Maximum pressure drop, overall efficiency for five different types of chimney design keeping the chimney height constant. The effect of solar intensity on output power is taken as other objective. Material cost of chimneys has been done to find the optimized chimney type which will give higher power output at lower cost.

3. WORKING PRINCIPLE OF SCPP:

The main components of the solar chimney power plant are shown in the Figure1. The main geometric parameters of the project are the height of the collector from the ground surface at entry($H_{coll} = 2m$), the height of the collector from the ground surface at the center($H_{coll} = 4m$),collector diameter ($D_{coll} = 258m$),chimney height($H_{ch} = 197m$) and chimney outlet diameter($D_{ch} = 10m$). The solar energy will penetrate the transparent solar collector and heat the ground surface and the around it. The hot air will move along the slant surface of the collector to the bottom of the chimney. This air while moving towards the open end of the chimney will pass through the turbine where the kinetic energy of the air will be converted to mechanical work. The generator coupled to the turbine will convert the mechanical work into electrical energy. Finally, the hot air will leave through the top of the chimney due to natural circulation and draught created by the chimney. A continuous air flow will be established from the entry of the collector (cold air) to the exit of the chimney(hot air). In the literature generally, three types of SCPP are found. They are a Basic type of chimney and convergent and divergent types of chimneys. Two new types of chimneys such as sudden expansion and sudden contraction are also considered in this paper for evaluation of performances which are shown in the Figure 1.

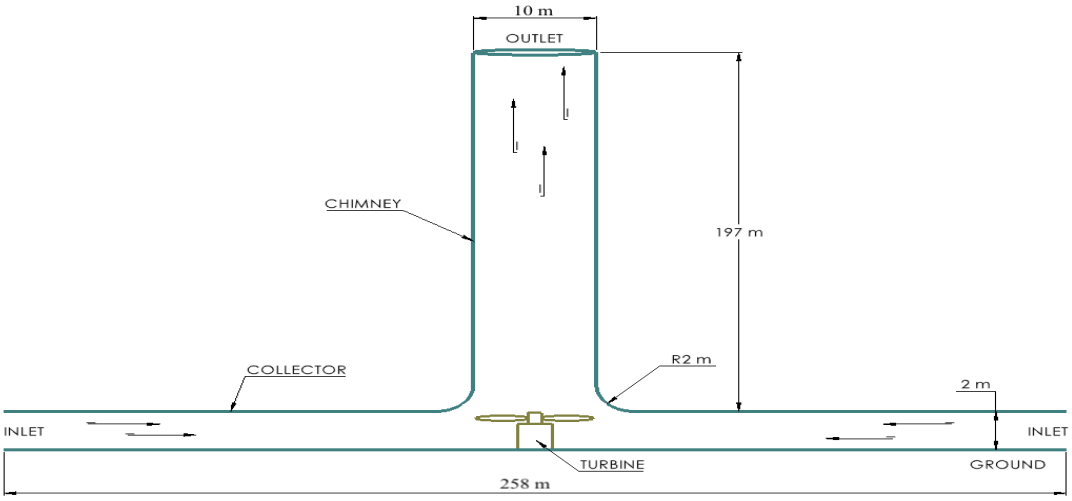

(a)**2D SCHEMATIC DIAGRAM OF SCPP**

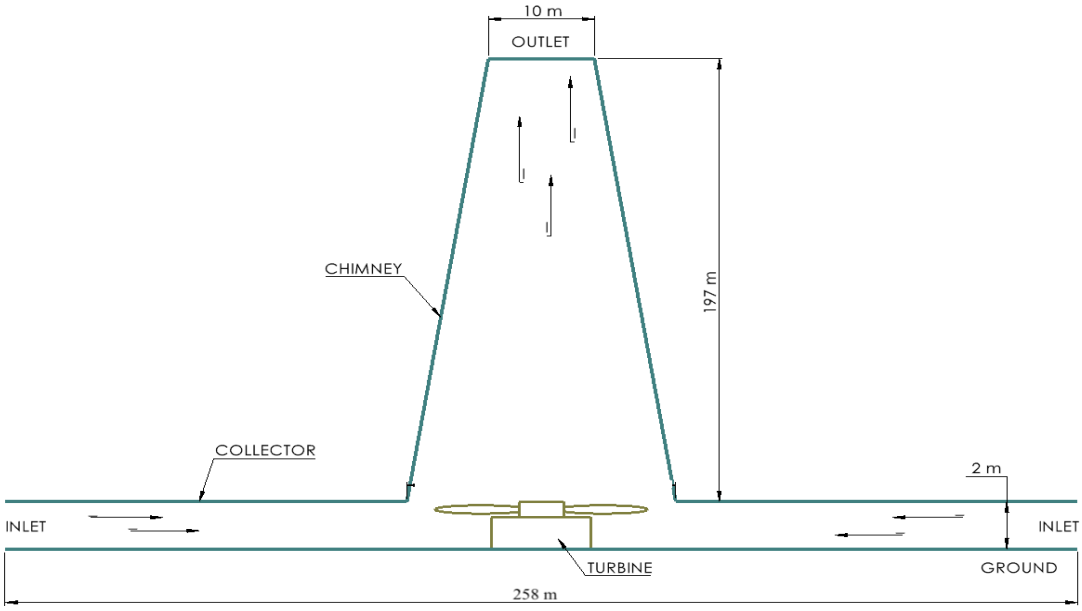

(b)**2D SCHEMATIC DIAGRAM OF CONVERGENT SCPP**

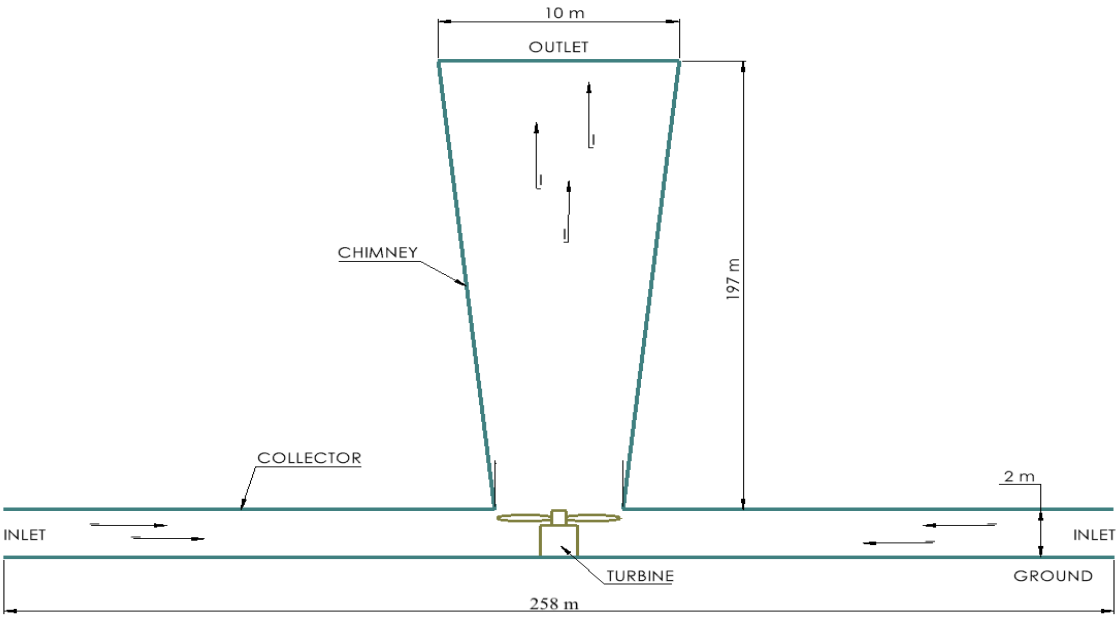

© 2D SCHEMATIC DIAGRAM OF DIVERGENT SCPP

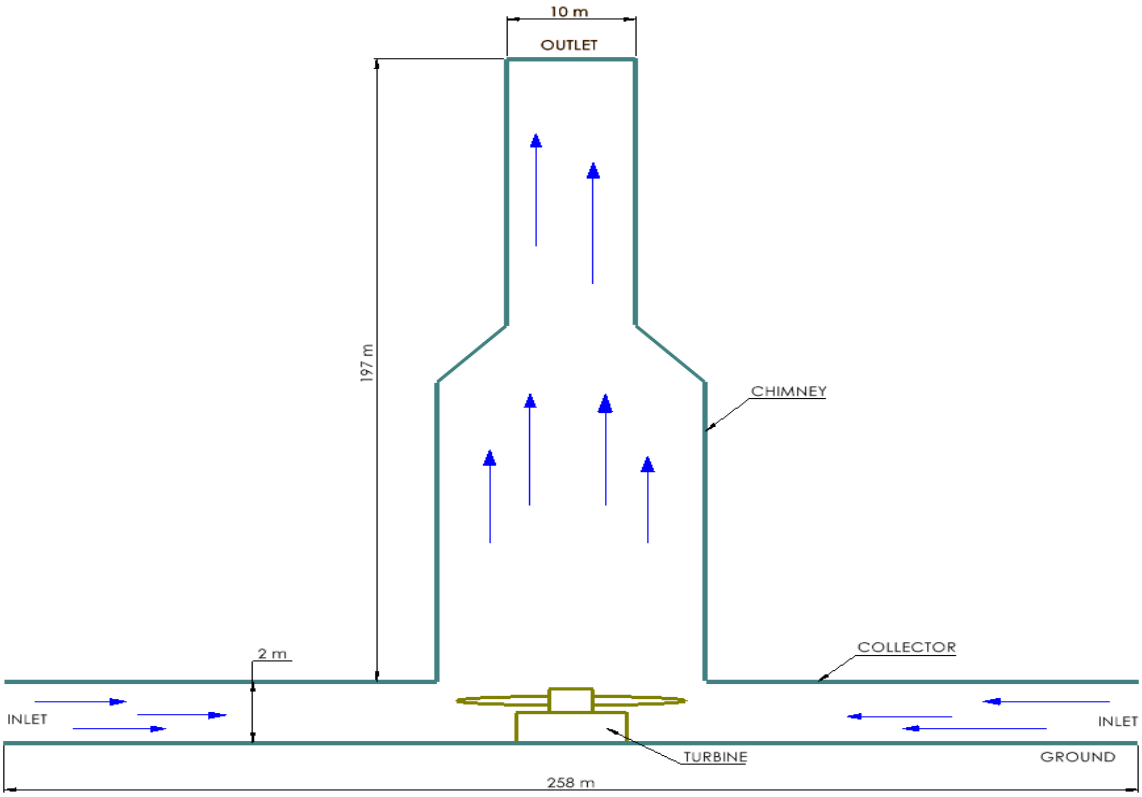

(d)2D SCHEMATIC DIAGRAM OF SUDDEN CONTRACTION SCPP

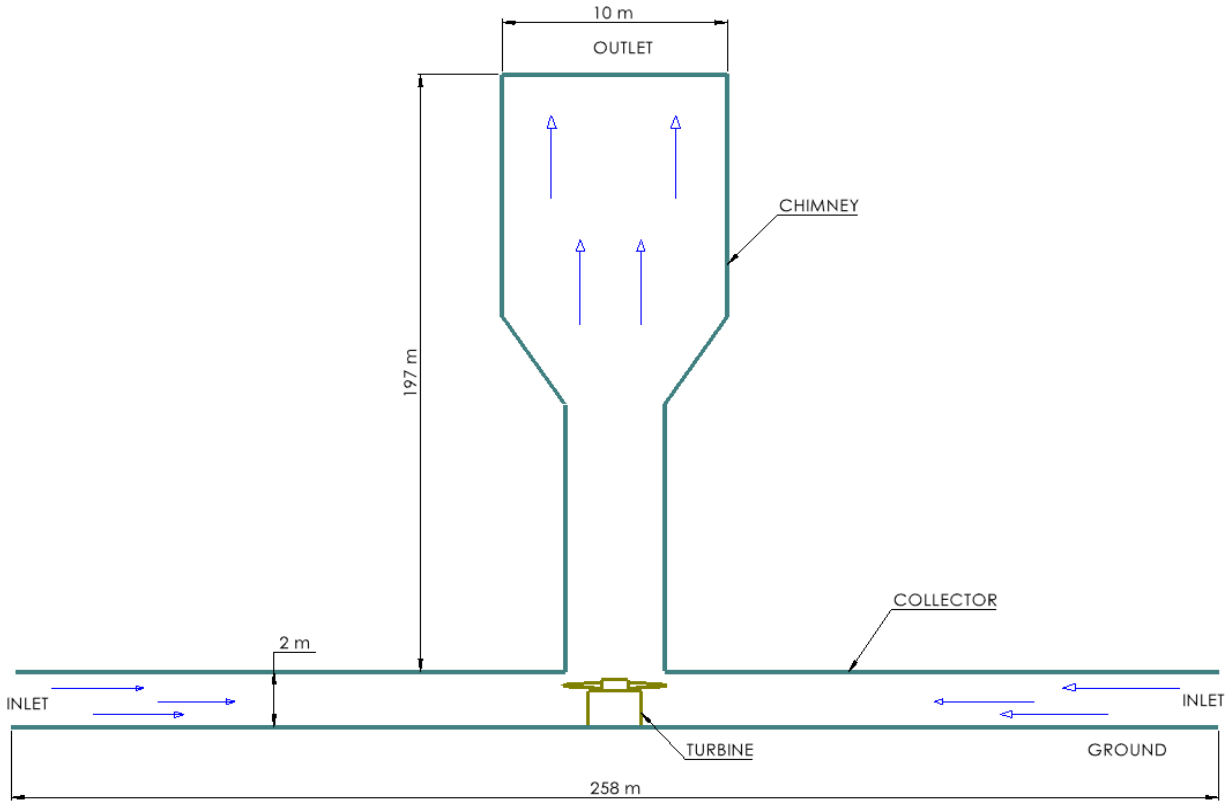

(e) **2D SCHEMATIC DIAGRAM OF SUDDEN EXPANSION SCPP**

Figure1. (a)2D SCHEMATIC DIAGRAM OF SCPP (b) 2D SCHEMATIC DIAGRAM OF CONVERGENT SCPP (c) 2D SCHEMATIC DIAGRAM OF DIVERGENT SCPP(d) **2D SCHEMATIC DIAGRAM OF SUDDEN CONTRACTION SCPP**(e) **2D SCHEMATIC DIAGRAM OF SUDDEN EXPANSION SCPP**

Lal et al. [22] have given a mathematical relation to calculate the total amount of power generated in a plant:

$$W_0=Q_s.\eta_0 \quad (1)$$

Where Q_s is the total amount of solar energy in the collector and η_0 is the overall efficiency of SCPP. The overall efficiency depends on the collector shape, chimney diameter, and height.

The thermal efficiency of the SCPP depends on the chimney efficiency. Guo et al. [23] added that the efficiency increases due to the buoyant effect that is causing the temperature and pressure variation at the top and base of the chimney. The relation of turbine power generation $P_{turbine}$ and heat flux in the collector $Q_{coll}$is given by the following equation:

$$\eta_{ch} = \frac{P_{turbine}}{Q_{coll}} \quad (2)$$

Hanna et al. [24] have described that the chimney in an SCPP is responsible for the conversion of heat flow by the collector (q_{added}) into the turbine work output ($p_{external}$) and that only determines the chimney efficiency. The chimney efficiency can be shown in relation:

$$\eta_{ch} = \frac{p_{external}}{q_{added}} \quad (3)$$

Lal et al. [22] have presented to determine the effect of chimney height on efficiency and the value of chimney efficiency can be obtained in percentage:

$\eta_{ch} = 0.0027H_{ch}^4 - 0.0347H_{ch}^3 - 0.1616H_{ch}^2 - 0.2868H_{ch} + 0.1775$ (4)

Maghrebi et al. [25] have stated that the efficiency of a chimney is the correlation of useful energy present in the airflow by turbine power output. Bouabidi et al. [26] have shown the velocity distribution inside the chimney. The velocity generated goes on to increase with the rise of the diameter of the chimney. Nasraoui et al. [27] have plotted a graph on the chimney efficiency rise vs chimney divergence radius and it shows that the rise is highest when the divergence radius is 15m.The above authors have already pointed out in detail the factors responsible for determining chimney efficiency.

4. METHOD:

The continuity equation is a fundamental principle in fluid dynamics that relates the mass flow rate of a fluid to its velocity and cross-sectional area within a conduit. In the context of designing a solar chimney power plant, the continuity equation can be applied to understand and optimize the airflow within the chimney structure, which is a key component of such a power plant.

Continuity equation:

$$\frac{\partial(\rho_{ui})}{\partial_{xi}} = 0 \quad (5)$$

Navier-Stokes equations can be applied to gain a deeper understanding of the fluid dynamics involved and to optimize the design and performance of the facility.

Navier-Stokes equation:

$$\frac{\partial(\rho u_i u_j)}{\partial_{xj}} = \rho g_i - \frac{\partial P}{\partial_{xi}} + \frac{\partial_{\tau ij}}{\partial_{xj}} \quad (6)$$

The energy equation can be used to model the heat absorption process within the solar collector.

Energy equation:

$$\frac{\partial(\rho C_p u_j T)}{\partial_{xj}} = \frac{\partial}{\partial_{xj}}(\lambda\frac{\partial T}{\partial_{xj}}) + \tau_{ij}\frac{\partial_{ui}}{\partial_{xj}} + \beta T(u_j\frac{\partial P}{\partial_{xj}}) \quad (7)$$

The problem is connected to natural convection, before solving the constitutive equation, it is essential to study the flow regime either in the laminar or turbulent zone. Rayleigh number (Ra) number determines the buoyancy-induced flow, which is governed by the following equation:

$$\mathrm{Ra} = \frac{g\beta\Delta T L^3\rho}{\mu\alpha} \quad (8)$$

Where ΔT and L define the maximum temperature difference of the airflow and average collector height respectively.$\beta$is the thermal expansion coefficient ($1/T_{max}$) and α is the thermal diffusivity ($k/\rho C_p$). Ra number value lies less than 10^8 in case of a buoyancy-driven laminar flow while the flow becomes turbulent in the range of 10^8<Ra<10^{10}. From the considered geometrical dimensions, the calculated value of Ra is more than 10^9, so the flow domain is in the turbulent regime.

The equation for the k-ε model:

$$\frac{\partial(\rho k_{ui})}{\partial_{xi}} = \frac{\partial}{\partial_{xj}}(\alpha k\mu_{eff}\frac{\partial k}{\partial_{xj}}) + G_k + G_b - \rho\varepsilon - YM + S_k \quad (9)$$

$$\frac{\partial(\rho\varepsilon_{ui})}{\partial_{xi}} = \frac{\partial}{\partial_{xj}}(\alpha\varepsilon\mu_{eff}\frac{\partial\varepsilon}{\partial_{xj}}) + C_{1\varepsilon}\frac{\varepsilon}{k}(G_k + C_{3\varepsilon}G_b) - C_{2\varepsilon}\rho\frac{\varepsilon^2}{k} - R_\varepsilon + S_\varepsilon \quad (10)$$

Where, G_k is the turbulence kinetic energy generation for mean velocity gradients. G_b is the turbulence kinetic energy generation for buoyancy. σ_T, σ_k and σ_ε represent the Prandtl numbers (turbulent) for T, k, and ε respectively: $\sigma_T = 0.9$, $\sigma_k = 1.0$, $\sigma_\varepsilon = 1.3$ and C1, C2 are two constants for turbulent model: C1 = 1.44, C2 = 1.92 and Cμ = 0.09.

Different modes of heat transfer need to be considered in a SCPP. Heat flux is generated from the solar radiation using the process of Ray Tracing and the results are merged with ANSYS FLUENT calculations. The obtained energy equation:

$$\frac{\partial}{\partial_t}(\rho E)+\nabla.(\vec{v}(\rho E)) = \nabla.((k_{eff}\nabla T - \sum_f h_f \vec{J}_f) + (\bar{\bar{\tau}}_{eff}.\vec{v})) + S_h \quad (11)$$

Where, S_h denotes the volumetric heat sources defined by the user, k_{eff} is the effective conductivity, $\vec{J}$ is defined as the diffusion flux of species j. If the flow is incompressible and no diffusion terms present then equation (11) can be modified as [28]:

$$\nabla.\left(\vec{v}(\rho E)\right) = \nabla.k_{eff}\nabla T + \bar{\bar{\tau}}_{eff}.\vec{v} + S_h\nabla.(\vec{v}(\rho E)) \quad (12)$$

$$\nabla.\left(\vec{v}(\rho E)\right) = \nabla.k_{eff}\nabla T + \bar{\bar{\tau}}_{eff}.\vec{v} + S_h \quad (13)$$

The radiative transfer equation for Discrete Ordinance (DO) model is given as: $\nabla.(I(\vec{r},\vec{s})\vec{s}) + (a+\sigma_s)I(\vec{r},\vec{s}) = an^2\frac{\sigma T^4}{\pi} + \frac{\sigma_s}{4\pi}\int_0^{4\pi} I(\vec{r},\overrightarrow{S'})\emptyset(\vec{s},\overrightarrow{S'})d\Omega'$ (14)

Where, I is the intensity of solar radiation, $\vec{r}$ is the position vector, $\vec{s}$ is the direction vector, T is the ambient temperature, $\overrightarrow{S'}$ is the scattering direction vector, $\emptyset$ is the phase function and Ω' is the solid angle.

Exergy is the useful energy that is utilized to transform into the power output of SCPP. Generally, the heat entering into the system and work going out of the system are taken as positive. Taking into account the first law of thermodynamics, for a process, the state 1 & 2 lie in equilibrium conditions:

$$\int_1^2 \delta Q - \int_1^2 \delta W = E_2 - E_1 \quad (15)$$

By integrate, we get:

$$Q_{1,2} - W_{1,2} = E_2 - E_1 \quad (16)$$

In the above equation (16), it is distinct that work and heat both are path dependent but energy change is not influenced by the path of the process and the solution is obtained directly from the final states of the system. By applying the second law of thermodynamics on the same system, we get:

$$\int_1^2 \frac{\delta Q}{T} \leq S_2 - S_1 \quad (17)$$

So, it is clear that heat transfer across the boundary (δQ) and its temperature (T) determines the entropy transfer between the closed system and the surroundings. In the exergy analysis, entropy generation is given by:

$$S_{gen} = S_2 - S_1 - \int_1^2 \frac{\delta Q}{T} \geq 0 \quad (18)$$

In the case of open loop systems, the mass transfer occurs through the openings apertures of the boundary, and mass, energy, and entropy are important parameters for thermodynamics. From the first law of thermodynamics defines the relation:

$$\sum_{in}\dot{m}(h+\frac{1}{2}V^2+gZ) - \sum_{out}\dot{m}(h+\frac{1}{2}V^2+gZ) + \dot{Q} - \dot{W}_{sh} = \frac{\partial E}{\partial T} \quad (19)$$

It should be kept in mind that the work transfer occurs generally in the form of a rotating shaft. In the above equations using the given second law of thermodynamics:

$$\sum_{in}\dot{m}s - \sum_{out}\dot{m}s + \frac{Q}{T} \leq \frac{\partial S}{\partial t} \quad (20)$$

The difference between equation (20) & equation (17) entropy transfer linked with the mass transfer across the boundary for closed systems. Due to this, the entropy generation can be calculated from the following relation:

$$\dot{S_{gen}} = \frac{\partial S}{\partial t} - \frac{\dot{Q}}{T} + \sum_{out}\dot{m}s - \sum_{in}\dot{m}s \geq 0 \quad (21)$$

Exergy can be also termed as the energy that is utilized to carry out a useful task. Exergy is zero as soon as the system and the surroundings gain an equilibrium condition. Assuming a constant value of specific heat C_p is shown in the relation:

$W_{max} = \dot{m}[(h - T_0 s)_{in} - (h - T_0 s)_{out}]$

$$W_{max} = \dot{m}[C_p \left(T_H - T_0 - T_0 ln \frac{T_H}{T_0}\right)] \quad (22)$$

It also symbolizes the deviation of the system from the reversible state and is shown as:

$$\eta_{II} = \frac{\dot{W}}{\dot{W}_{max}} = 1 - \frac{\dot{W}_{lost}}{\dot{W}_{max}} \quad (23)$$

Utilizing equation (21):

$$\dot{W}_{lost} = T_0 \dot{S}_{gen} \quad (24)$$

This equation (24) is known as Gouy-Stodola theorem. There should not be any confusion of equation (23) with the first law of efficiency, which signifies heat engine working between heat reservoirs T_H and T_L is shown by:

$$\eta_I = \frac{W}{Q_H} = \eta_{II} \left(1 - \frac{T_L}{T_H}\right) = \eta_{II} \eta_{carnot} \quad (25)$$

The collector efficiency with surface area $A = \pi r^2$ is given by:

$$\eta_{coll} = \frac{Q}{AG} \quad (26)$$

Where, Q is the generated heat because of the greenhouse effect and is given by:

$$Q = C_p.m.\Delta T \quad (27)$$

Where, m ($\rho_{air}.V_{ch}.A_{ch}$) is the mass flow, V_{ch} is the velocity, $A_{ch}$is the inlet surface area of the chimney. By substituting the expressions Q and m in equation (26):

$$\eta_{coll} = \frac{m.C_p.\Delta T}{AG} \quad (28)$$

$$\eta_{coll} = \frac{\rho_{air}.V_{ch}.A_{ch}.C_p.\Delta T}{\pi r^2 G} \quad (29$$

The pressure difference between the inlet and outlet of the collector can be established from the following relation given by Cao et al. [29]:

$$\Delta P = \int_{inlet}^{outlet} g \left(\rho_{air} - \rho(z)\right) dz \quad (30)$$

Where, z is the height.

The equation for calculating the efficiency of a chimney is given by:

$$\eta_{ch} = \frac{g.H_{ch}}{C_p.T_a} \quad (31)$$

Therefore, chimney efficiency varies directly to the ratio between chimney height (H_{ch}) and the surrounding temperature (T_a). Where H_{ch} represents chimney height, the flow power (P_{tot}) is designated as:

$$P_{tot} = \frac{g_{ch}.H_{ch}}{T_a} \rho_{coll}.V_{ch}.\Delta T.A_{ch} \quad (32)$$

There is a pressure drop in the chimney is:

$$\Delta P_{tot} = \rho_{coll} g H_{ch} \frac{\Delta T}{T_a} \quad (33)$$

The expression of mechanical power utilized by the turbine is depicted by Sangi [30]:

$$P_m = \frac{2}{3} \eta_{coll} \eta_{ch} A_{coll} G \quad (34)$$

The above equation (34) can be further modified as:

$$P_m = \frac{2}{3} \eta_{coll} \eta_{ch} \pi r^2 G \quad (35)$$

For different dimensions, the efficiency of the turbine lies in the range of 0.8 to 0.9. Considering the performance study of different SCPP the value is taken as 0.83. The electric power generated is given by the expression:

$$P_e = \frac{2}{3}\eta_{coll}\eta_t \frac{g}{C_p.T_a} H_{ch}\pi r^2 G \quad (36)$$

The potential power output available in the turbine is given by the equation used by [29]:

$$P_{tot} = \Delta p_t.Q_v \quad (37)$$

Where, Δp_t is the pressure drop in the turbine and Q_v is volumetric from. The shaft power can be obtained from the rpm and torque of the rotor:

$$P_t = \frac{2\pi n_t M}{60} \quad (38)$$

Where, n_t is the rotational speed and M is the torque acting. From equation (37) & (38), we get the equation of turbine efficiency (η_t):

$$\eta_t = \frac{P_t}{P_{tot}} \quad (39)$$

The overall efficiency of the plant can be evaluated by the relation used by Gholamalizadeh and Kim [31]:

$$\eta_{scpp} = \eta_{coll}.\eta_{ch}.\eta_t \quad (40)$$

The data on the performance and operation of the Manzanares STC prototype was obtained from [2] along with the data present on outside temperature and material characteristics. It has been noted that the generated power is 27 kw to 35 kw with the atmospheric temperature ranging from 297 k to 309 k. The power recorded is found to be 5% to 9% less than the recorded power generation which proves that the data obtained is accurate.

By observing the above equations, it can be verified that several factors are responsible for electric power generation. These are both geometrical configurations diameter of the collector, height and diameter of the chimney, space between the ground and collector roof and atmospheric changes that ambient temperature, incident solar radiation and atmospheric pressure.

4.1 NUMERICAL PROCEDURE:

The present study is carried out numerically using the finite volume based reliable commercially available ANSYS-Fluent 18.1 solver. Here, the 30^0 CFD model is used and preferred to shorten the total iteration period instead of the whole geometry. The SIMPLE algorithm technique is used for the solution. For obtaining the converged solution, a minimum criterion of 10^6 is chosen for the computation.

4.1.1 Discretization technique:

Gradient: Green Gauss cell based
Pressure: PRESTO
Momentum: Second order upwind
Turbulent kinetic energy: Second order upwind
Turbulent dissipation rate: First order upwind
Energy: Second order upwind
Discrete ordinates: First order upwind
Under relaxation factor:
Pressure: 0.3
Momentum: 0.8
Turbulent kinetic energy: 0.8

Turbulent dissipation rate: 0.8

4.1.2 Boundary Conditions:

Inlet**:** Inlet Pressure has been taken as 0-gaugepressureand Temperature= 302K
Outlet: Outlet pressure is taken as 0-gauge pressure and temperature =302K
Collector (Transparent Cover): Heat transfer coefficient= 10W/m^2K, Temperature= 302K
Ground Surface (Absorber Plate): Heat flux= 0W/m^2
Chimney (Adiabatic wall): Thickness= 0.00125m
For predicting the correct results, a mesh sensitivity test of the SCPP geometry is carried out exhaustively for the different grid sizes with different element sizes using constant solar radiation of 1000 W/m^2. The results are compared using the extreme temperature, velocities, velocity at the chimney base, temperature, and rate of mass flow. The mesh size is chosen as M (73862) for the element size 0.80 respectively, which are presented in Table2. The cumulative error in the consecutive grid decrease as element size becomes smaller and finally, M is used for the study due to changes in the values being very less. As the shape changes due to modification of the ground absorber surface, the grid size is finalized by taking 0.8 element size for further study of different modified models. Details about the mesh structure used in the computational model for the modified SCPP are presented in below Figure2, Figure 3, Figure 4 and Figure 5with 3D view of the SCPP model,30^0CFD model with a cylindrical coordinate system, and an enlarged view of the chimney base area.

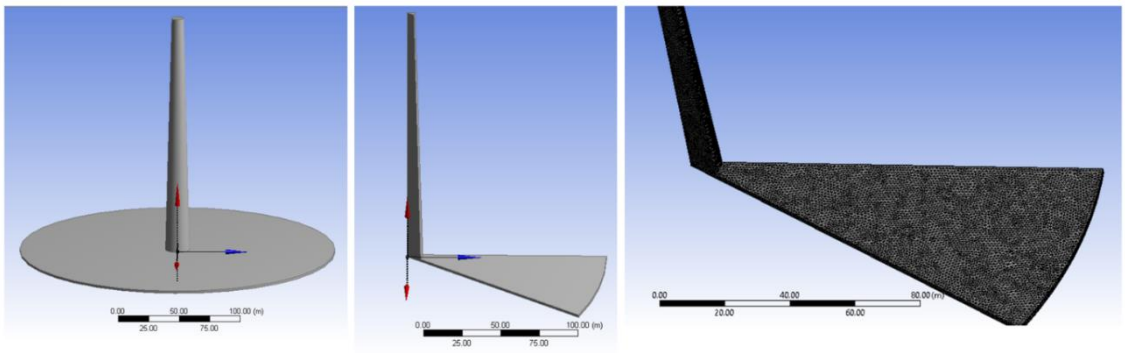

(a) (b) (c)

Figure 2: Mesh generation for the modified Convergent SCPP: (a) 3D view of the SCPP model, (b) 30^0 CFD model with a 3D coordinate system, (c) enlarged view of the chimney base area.

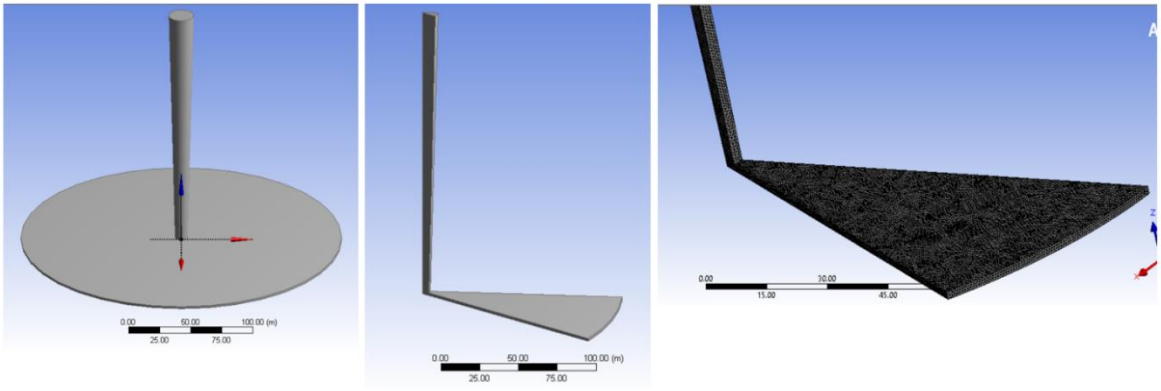

(a) (b) (c)

Figure 3: Mesh generation for the modified Divergent SCPP: (a) 3D view of the SCPP model, (b) 30^0 CFD model with a 3D coordinate system, (c) enlarged view of the chimney base area.

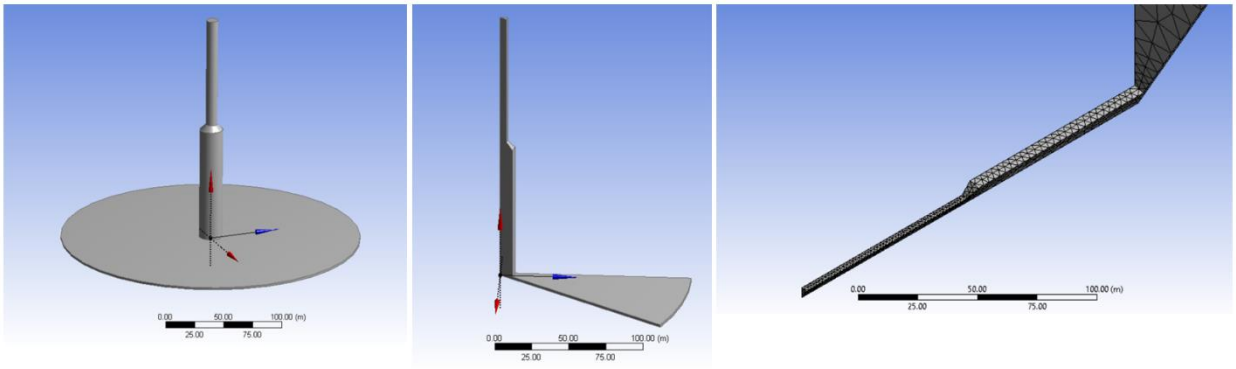

(a) (b) (c)

Figure 4: Mesh generation for the modified Sudden contraction SCPP: (a) 3D view of the SCPP model, (b) 30^0 CFD model with a 3D coordinate system, (c) enlarged view of the chimney base area.

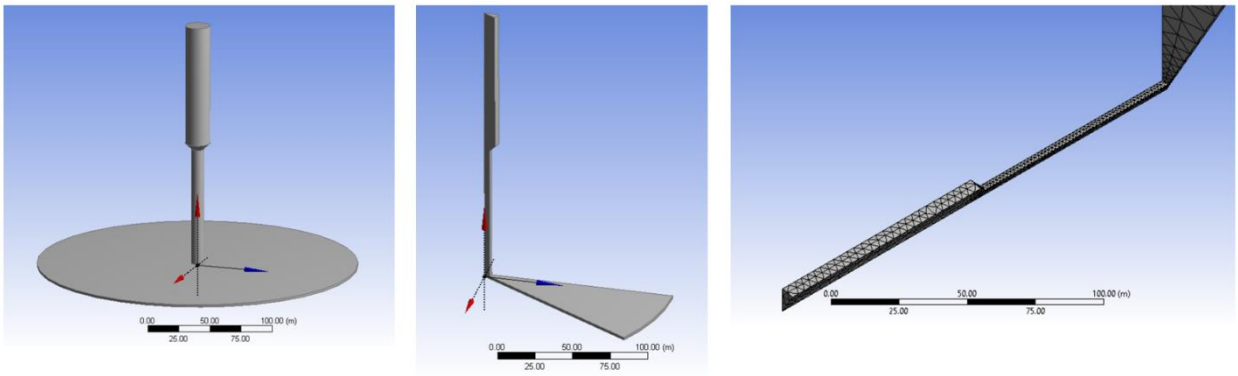

(a) (b) (c)

Figure 5: Mesh generation for the modified Sudden expansion SCPP: (a) 3D view of the SCPP model, (b) 30^0 CFD model with a 3D coordinate system, (c) enlarged view of the chimney base area.

5. ANALYSIS OF RESULTS:

Performance enhancement is the main concern of any study in SCPP. Five types of chimney design namely Base type, divergent, convergent, sudden contraction and sudden expansion are taken for analysis of performance so that optimum chimney design can be obtained. Pressure distribution especially at the turbine inlet is of vital importance to assess the performance of any plant based on SCPP. The velocity distribution is another component to know the volume flow rate for obtaining the power developed by the plant. Air temperature has a major impact on air velocity. Considering all these phenomena, this subsection examines the flow parameters like velocity, pressure, temperature, and to get an insight into the flow physics of the SCPP model. Since the collector outlet is the proper location for achieving the maximum results of buoyant convection due to the solar radiation effect, the chimney base is taken as a reference to examine the pressure, temperature, and velocity distribution as shown in the Figure6-9below. Figure 6 shows the pressure drop , velocity of air and temperature rise of convergent chimney, similarly for divergent chimney in Figure 7 , sudden contraction in Figure8 and sudden expansion in Figure 9. Power output of five types of chimneys have been calculated. Power output of basic chimney at different solar intensity has been calculated. The data are shown in figure 11. With increase of solar Intensity power

output increases which is shown in Figue11. When compared with the literature data the results has been found to be comparable. Literature data are given in table 3-5.

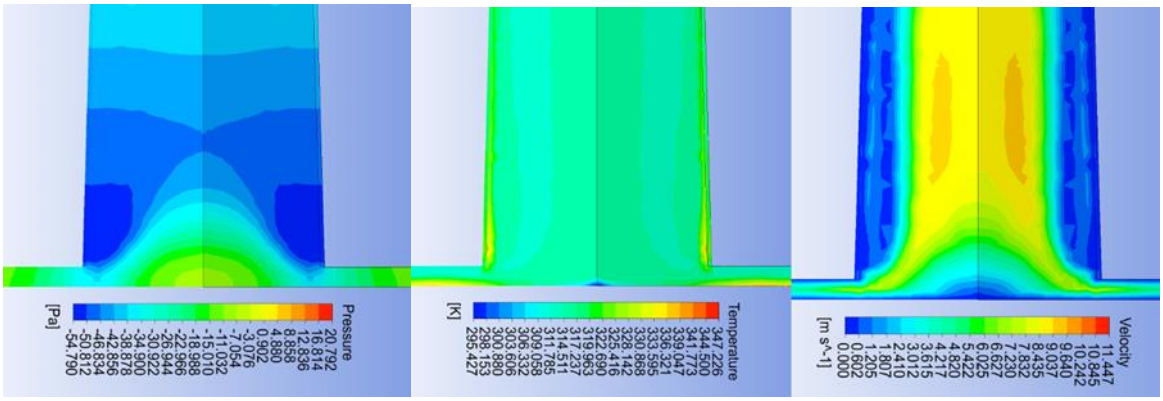

Figure 6: Convergent

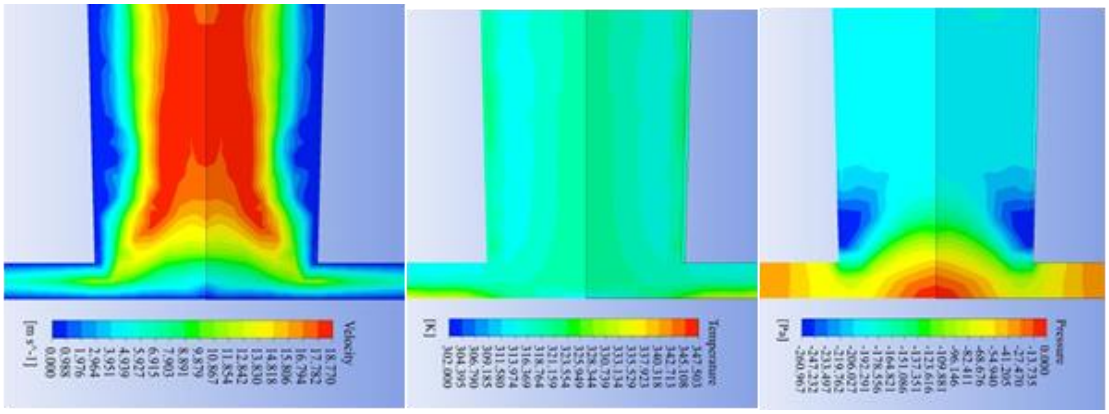

Figure7: Divergent

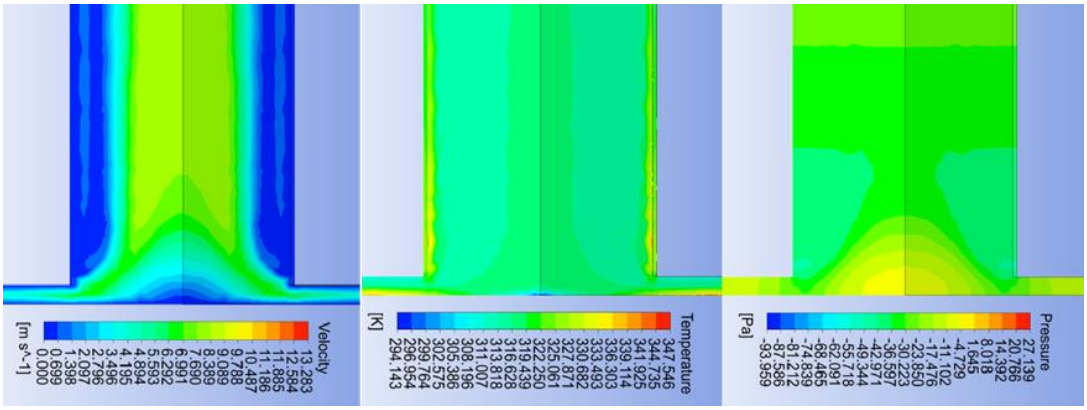

Figure8: Sudden Contraction

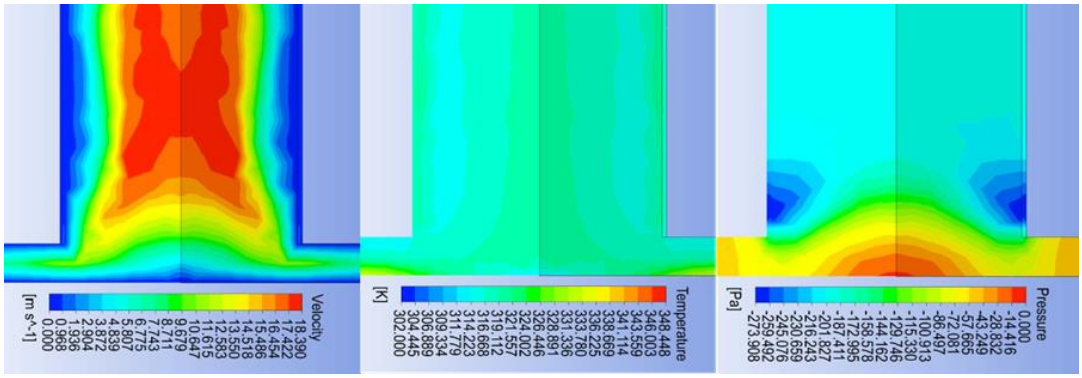

Figure9: Sudden Expansion

Table 1: Thermophysical Properties of Air, Collector, Ground Absorber, and Chimney:

Properties	Air	Collector	Ground Absorber	Chimney
Material	Air[32]	Glass	Iron	Aluminum
Density (ρ)kg/m^3	1.2046	2500	2183	2710
Specific heat (C_p)J/kg/K	1006.43	750	996	880
Thermal conductivity (K), W/mK	0.0259	1.15	2	1.4
Absorptivity	0.85	0.03	0.9	1.0
Transmissivity	0.64	0.9	Opaque	Opaque
Thermal expansion coefficient (β),K^{-1}	3.31X10^-3/K	6.7X10^-7/K	-	23.5X10^-6/K
Thickness, m	-	0.004	0.5	0.00125
Refractive index	1.0003	1.526	1.0	1.0
Emissivity	0.85	0.1	0.9	1.0

Table 2: Mesh Sensitivity Test using the Maximum Velocity, Temperature, Chimney Base Velocity and Temperature and Mass Flow Rate:

	Mesh size/Element size (M)73,862			
Parameters Checked	**Convergent**	**Divergent**	**Sudden expansion**	**Sudden contraction**
Max Velocity	11.44	18.77	18.39	13.28
Max Temperature	347.54	348.44	349.12	348.10
CB Velocity	9.87	11.13	11.10	8.04
CB Temperature	314.99	317.05	317.67	316.05
Mass Flow Rate	32.57	24.23	23.13	28.67

Table 3: Comparison of the present results with the published results using chimney base velocities.

Published literature	Experimental/Numerical study	Chimney Base Velocity(m/s)
Present study	Numerical	Convergent- 9.87 Divergent- 11.13
Biswas et al. [33]	Numerical	10.47
Haaf et al. [2]	Experimental	9.00
Koonsrisuk and Chitsomboon [34]	Numerical	7.25

Gholamalizadeh and Kim [31]	Numerical	9.10
Guo et al. [35]	Numerical	8.20
Keshari et al. [36]	Numerical	9.87

Table 4: Comparison of the present results with published results using temperature rise.

Published literature	**Experimental/Numerical study**	**Temperature rise(K)**
Present study	Numerical	Convergent- 18 Divergent- 19.08
Biswas et al.[33]	Numerical	17
Haaf et al. [2]	Experimental	20
Koonsrisuk and Chitsomboon [34]	Numerical	17.8
Sangi et al. [37]	Numerical	20.96
Kasaeian et al. [38]	Numerical	18.8

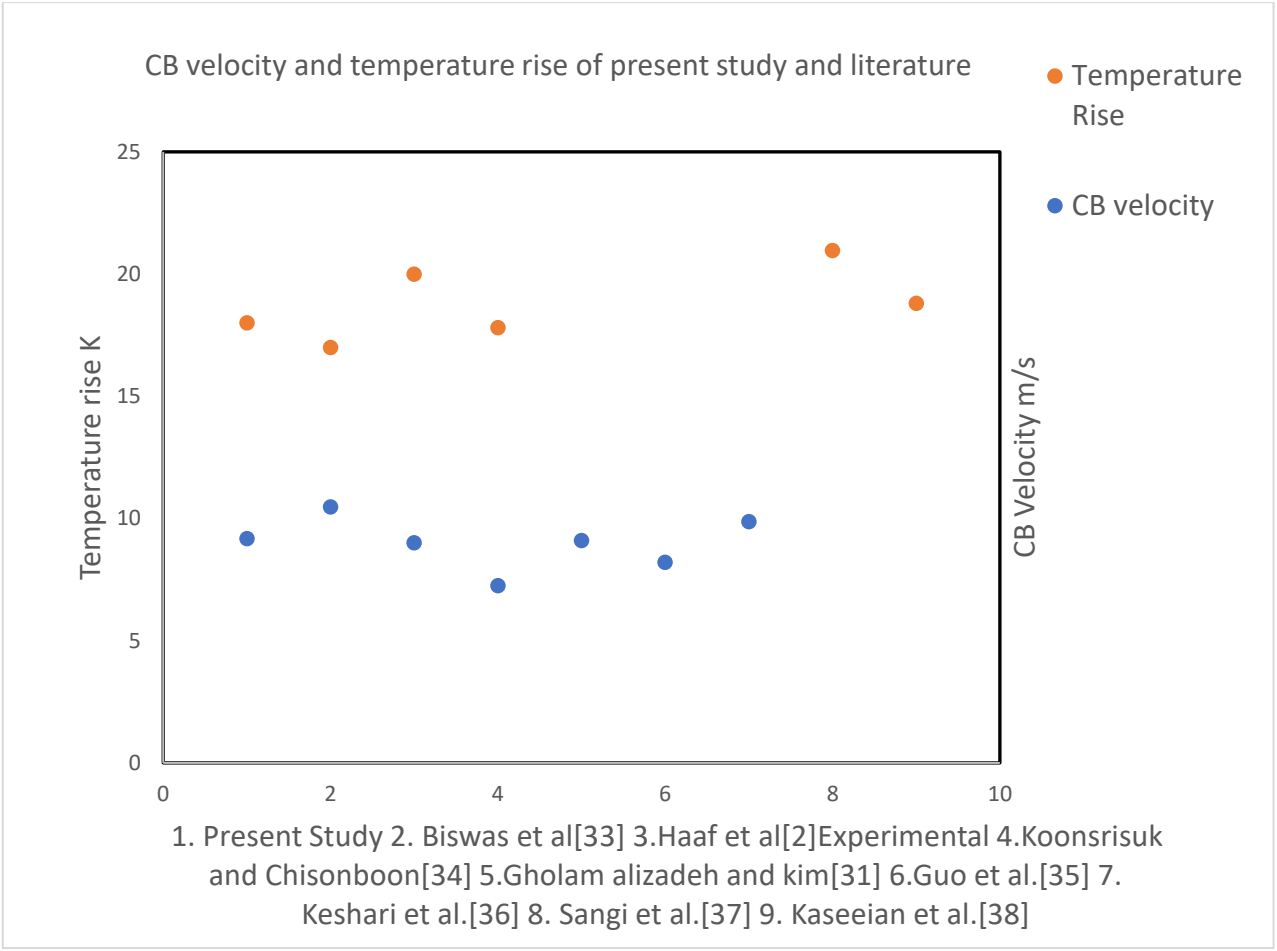

Figure 10: CB velocity and temperature rise of present study and literature

Table 5: Comparison of the present results with published results using power produced (P_{act}).

Solar intensity (kW/m^2)	The present study (Numerical)	Biswas et al. [33] (Numerical)	Haaf et al. [2] (Experimental)	Cuce [39] (Numerical)	Keshari et al. [36] (Numerical)
0.4	Convergent-26 Divergent-30	20	-	19.451	-
0.6	Convergent-36 Divergent-40	30	-	30.742	-
0.8	Convergent-48 Divergent-52	42	-	42.445	-
1.0	Convergent-58 Divergent-60	52	50	54.478	56

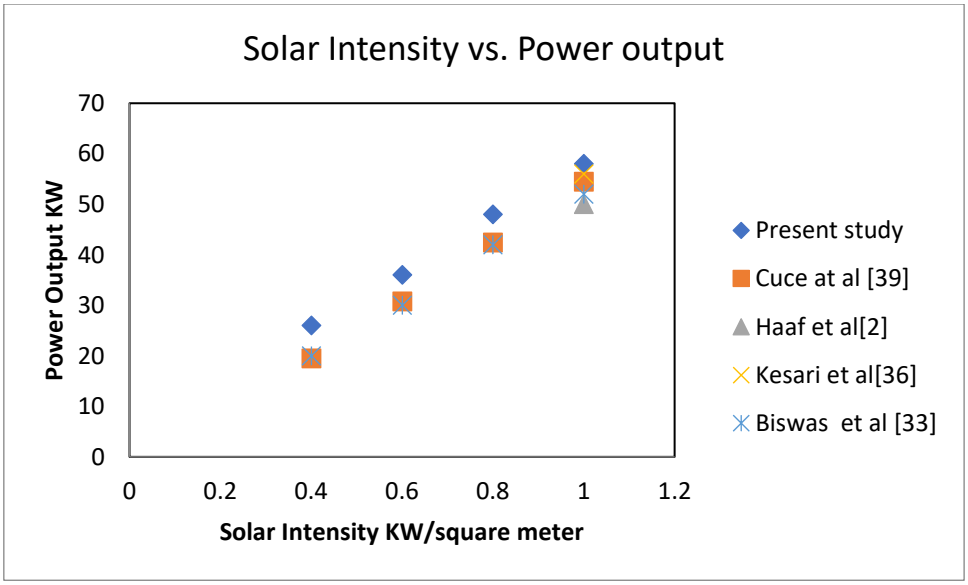

Figure11: Solar Intensity vs. power output

Fitting curves using developed correlations for the original data versus predicted data with regression coefficients for power, collector efficiency, overall chimney efficiency, max velocity, max temperature, CB velocity, CB Pressure, CB Temperature, and Pressure Drop. Power output of divergent and sudden expansion chimneys are higher than others (Figure12). In Divergent type of Chimney, gradual expansion of the chimney allows for a smoother flow transition, reducing pressure losses and turbulence. It can help improve the overall efficiency of the chimney system. Sudden expansion chimneys are effective in reducing exit velocities significantly. The sudden increase in flow area converts kinetic energy into

pressure energy, increasing static pressure at the chimney exit. Materials requirement for sudden expansion type of chimney is less than divergent type of chimney. Because diameter increase is from a height of 2/3 rd of the chimney height for a sudden expansion type of chimney. Collector efficiency of convergent and sudden contraction are higher than others(Figure 13). It is obvious that there is velocity reduction and retention time for air is more. Overall efficiency of divergent and sudden expansion type of chimney are higher than others (Figure14). Maximum velocity of divergent and sudden expansion are higher than others (Figure15). By gradually widening or having sudden expansions, these chimney designs can reduce the pressure losses that occur due to fluid friction. This means that the exhaust air can flow more smoothly through the chimney, reducing energy losses in the process. In a divergent chimney, the gradual increase in cross-sectional area can aid in better dispersion of air. This can help prevent backflow or recirculation of gases, which would otherwise hinder the efficiency of the chimney. An optimized designs of these chimneys can lead to a reduction in backpressure on the source of the air. Lower backpressure allows the source to operate more efficiently, leading to improved overall system efficiency. A well-designed divergent or suddenly expanding chimney can create a better draft effect. The draft effect is the flow of air caused by the temperature difference between the inside and outside of the chimney. An improved draft effect can result in lower losses.Maximum temperature of sudden expansion and divergent chimneys are higher than Others (Figure16). Both divergent and sudden expansion chimneys, as described earlier, can contribute to better efficiency and less pressure losses, which could result in a higher retention of heat and maintain elevated temperatures. A well-designed divergent or suddenly expanding chimney can be help prevent backflow or recirculation of flue gases. This reduces the possibility of cooled air leaving, mixing with the hot upcoming air, thus preserving the high temperature of the flue gases. CB velocity of sudden expansion and divergent chimneys are higher than others (Figure17). A sudden expansion chimney design allows the air to rapidly expand as it exits the collector and enters the chimney. This expansion leads to an increase in velocity. The sudden expansion creates a pressure difference between the collector and the chimney, causing a natural draft effect. This draft effect enhances the airflow velocity. The higher velocity at the collector base enables a greater volume of air to be drawn into the chimney, which can lead to more efficient power generation. A divergent chimney design gradually widens as it extends upward. This design helps in converting the thermal energy of the hot air collected in the solar chimney to kinetic energy (velocity) more efficiently. The gradual increase in cross-sectional area allows the air to expand and accelerate as it moves up the chimney, resulting in higher velocities. The divergent chimney design can create a better venturi effect, where the narrowing of the chimney at the top further increases the velocity of the airflow. Higher base velocity in a divergent chimney increases the airflow rate, which can improve power generation in the solar chimney power plant. It's essential to note that the collector base velocity is crucial for the overall efficiency of a solar chimney power plant. A higher velocity at the collector base means that more air is being drawn into the chimney, resulting in increased airflow and greater power generation potential. However, other factors, such as the collector design, chimney height, and solar radiation intensity, also play significant roles in determining the overall performance of the solar chimney power plant. CB temperature of sudden expansion and divergent chimneys are higher than others (Figure18). In a Solar chimney power plant, the collector base temperature refers to the temperature of the air at the base of the solar collector. The temperature at this point is influenced by several factors, including solar radiation, ambient temperature, collector design, and chimney configuration.The sudden expansion chimney design allows for efficient mixing of the incoming air with the hot air collected in the solar collector. As the hot air expands and exits the collector, it rapidly mixes with the incoming cooler air,

leading to an increase in temperature. The rapid mixing and higher velocity in the sudden expansion chimney design help reduce heat losses and enhance the transfer of thermal energy from the solar collector to the airflow. The higher base temperature in a sudden expansion chimney indicates that the collector is effectively capturing and retaining solar heat, making it more efficient in converting solar energy into thermal energy. The divergent chimney design also aids in efficient mixing of the hot air collected in the solar collector with the incoming air. As the air moves up the divergent chimney, it gradually expands, leading to higher temperatures. The gradual expansion in the divergent chimney allows for a longer contact time between the hot air and the incoming air, facilitating better heat transfer and raising the base temperature. The improved mixing and higher base temperature of the divergent chimney contribute to increased thermal efficiency and overall power generation potential of the solar chimney power plant.CB pressure of sudden expansion and divergent chimneys are higher than others(Figure19). The collector base pressure refers to the air pressure at the base of the solar collector. The pressure at this point is influenced by various factors, including solar radiation, collector design, chimney configuration, and the surrounding atmospheric conditions. The sudden expansion chimney design creates a pressure difference between the collector and the chimney. As the hot air collected in the solar collector rapidly expands and exits into the chimney, it creates a higher pressure at the collector base. The sudden increase in cross-sectional area at the exit of the collector causes a pressure drop, resulting in a higher-pressure gradient and consequently higher base pressure. The higher base pressure in a sudden expansion chimney helps drive the airflow upwards through the chimney, increasing the flow rate and improving the overall efficiency of the solar chimney power plant. The divergent chimney design allows for gradual expansion of the hot air collected in the solar collector as it moves up the chimney. This expansion process leads to a higher pressure at the base of the collector. The gradual expansion in the divergent chimney design results in a smoother pressure transition, reducing pressure losses and maintaining a higher base pressure. The higher base pressure in a divergent chimney contributes to a better draft effect, helping to draw more air into the system and increasing the airflow rate through the chimney. Pressure drop of sudden expansion and divergent chimneys are higher than others (Figure20). The pressure drop refers to the decrease in air pressure as the air flows through the system, from the collector base to the chimney exit. The pressure drop is an important consideration as it affects the overall efficiency and performance of the power plant. In a sudden expansion chimney, the air rapidly expands as it exits the collector and enters the chimney. This sudden expansion creates a pressure drop at the exit of the collector. The pressure drop in the sudden expansion chimney is more pronounced due to the abrupt increase in cross-sectional area. The pressure drop is associated with an increase in air velocity, which is required for efficient power generation in the chimney. While the higher- pressure drop helps drive the airflow upwards through the chimney, it can also lead to higher friction losses and result in a more significant reduction in pressure along the flow path. In a divergent chimney, the air gradually expands as it moves up the chimney. The gradual expansion is designed to convert thermal energy into kinetic energy (velocity) more efficiently. While the pressure drop in a divergent chimney is generally less abrupt than in a sudden expansion chimney, it is still present due to frictional losses and the gradual increase in cross-sectional area. The pressure drop in a divergent chimney is associated with the increase in airflow velocity and the improvement of the chimney's draft effect. Sudden expansion can potentially help increase the speed of the updraft, leading to higher energy conversion. However, it’s essential to balance the design to avoid excessive turbulence or pressure drops that could reduce efficiency. A sudden expansion type of chimney may be advantageous from the point of view of increased air, reduced flow resistance and enhanced mixing but on the other hand an improper

design could lead to unintended consequences such as flow separation, turbulence, or reduced updraft velocity. A sudden expansion type of chimney involves engineering challenges in terms of structural integrity, materials, and construction methods to accommodate the change in chimney diameter. The actual gains of such type of chimney might vary depending on factors such as local climate conditions, collector design, and turbine efficiency. The cost of design, construction and maintenance of sudden expansion type of chimney may be higher than a basic type of chimney which could be concluded only after proper analysis. It's essential to conduct through simulations, modeling, and testing to ensure that the sudden expansion will indeed lead to improved performance and justify the additional cost and complexity.

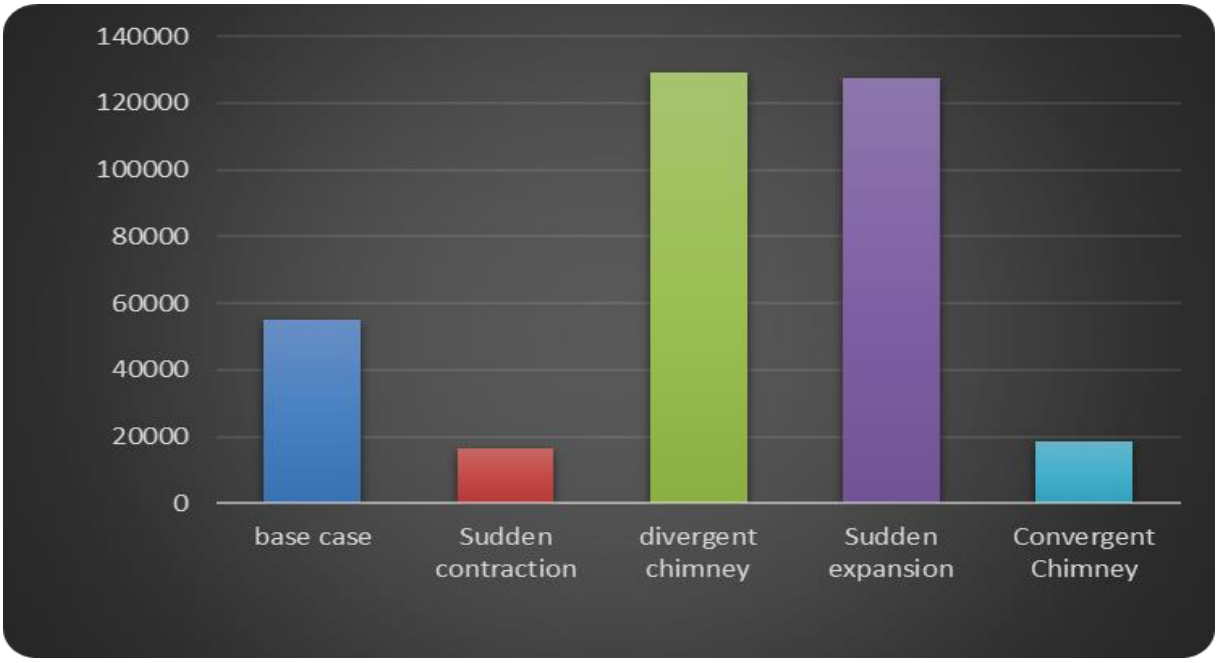

Figure12: Poweroutput of different chimney(W)

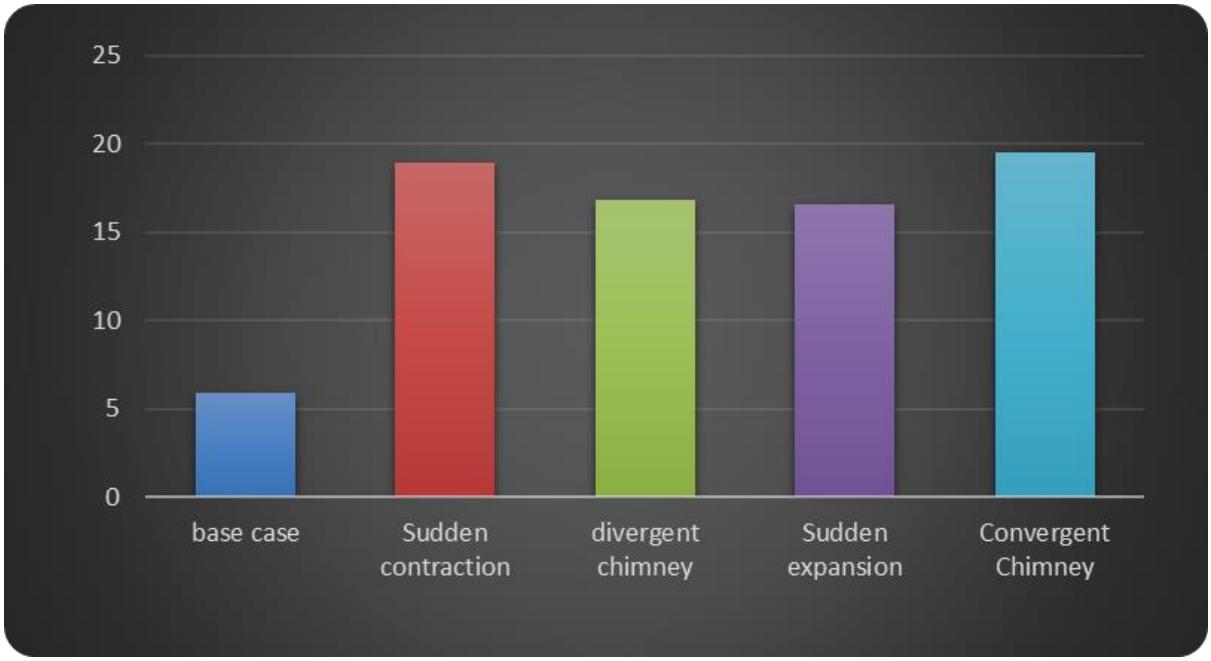

Figure 13:η_c,Collector Efficiency of different chimney (%)

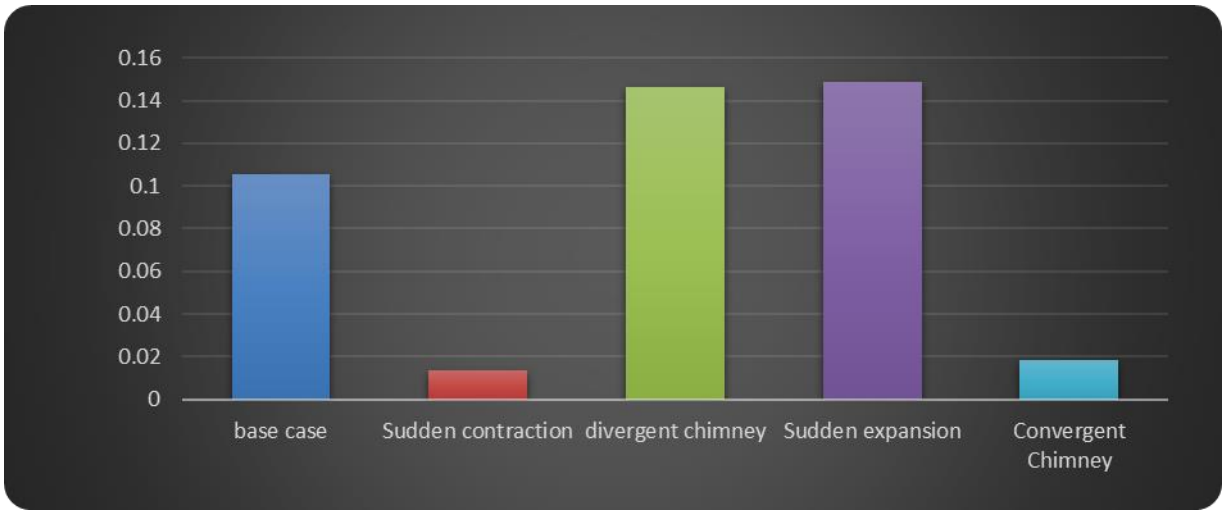

Figure 14:η_o Overall Efficiency of different chimney

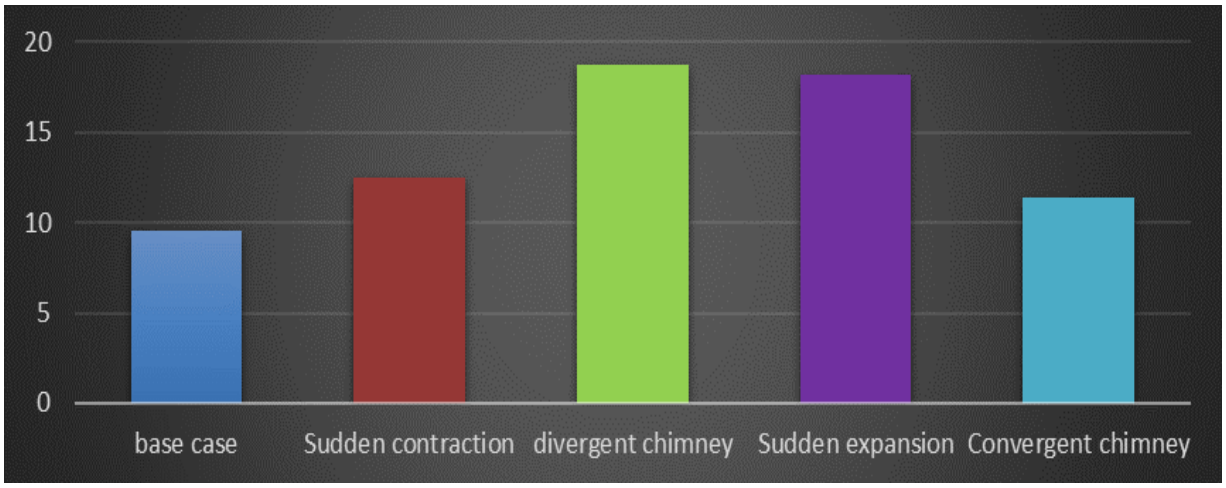

Figure 15: Max Velocity of different chimney(m/s)

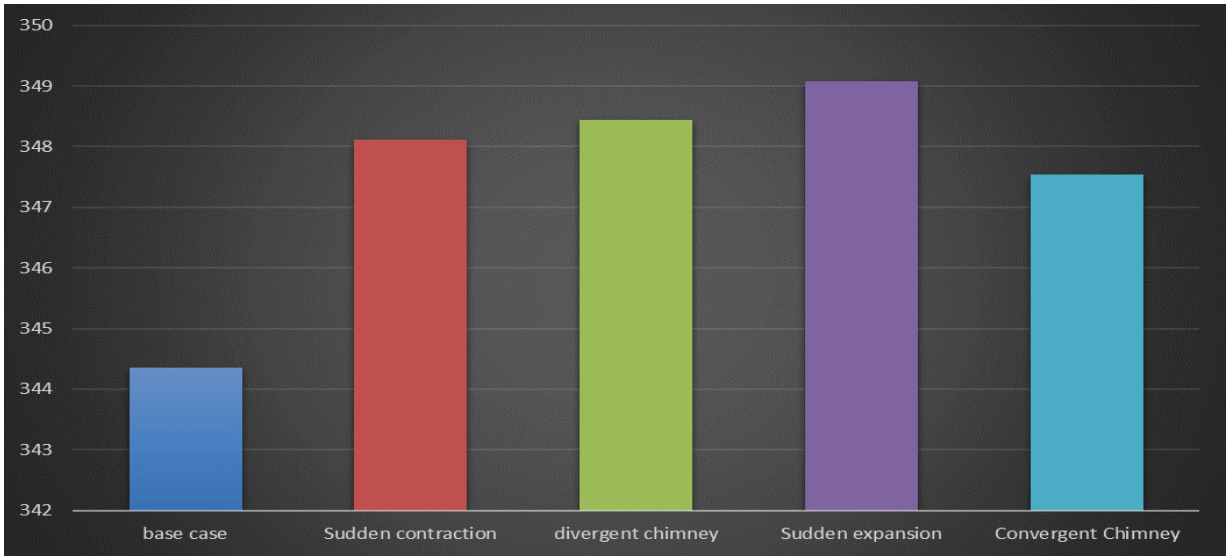

Figure 16: Max Temperature of different chimney(K)

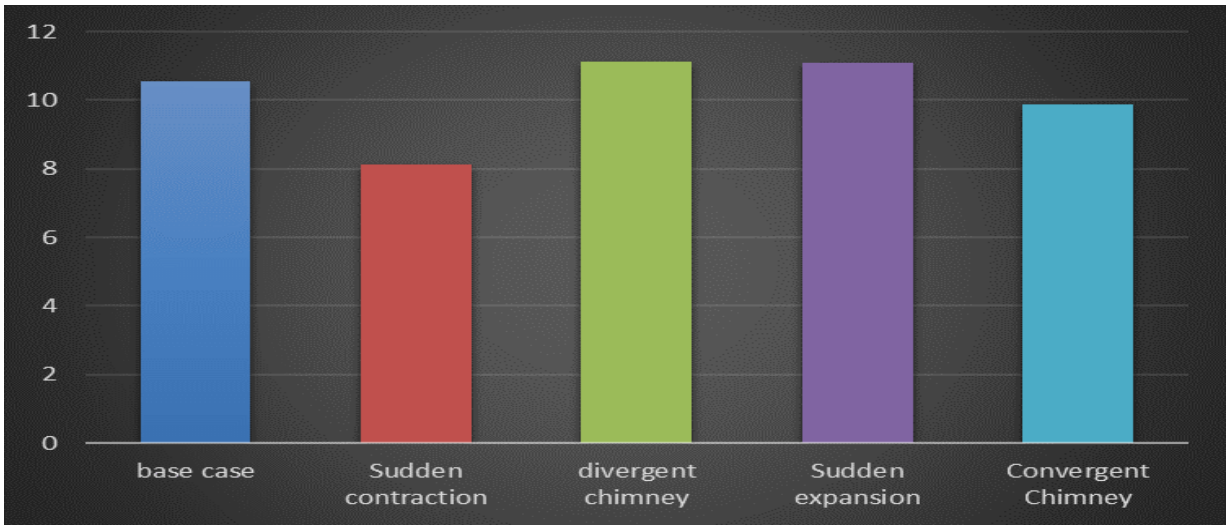

Figure 17: CB Velocity of different chimney(m/s)

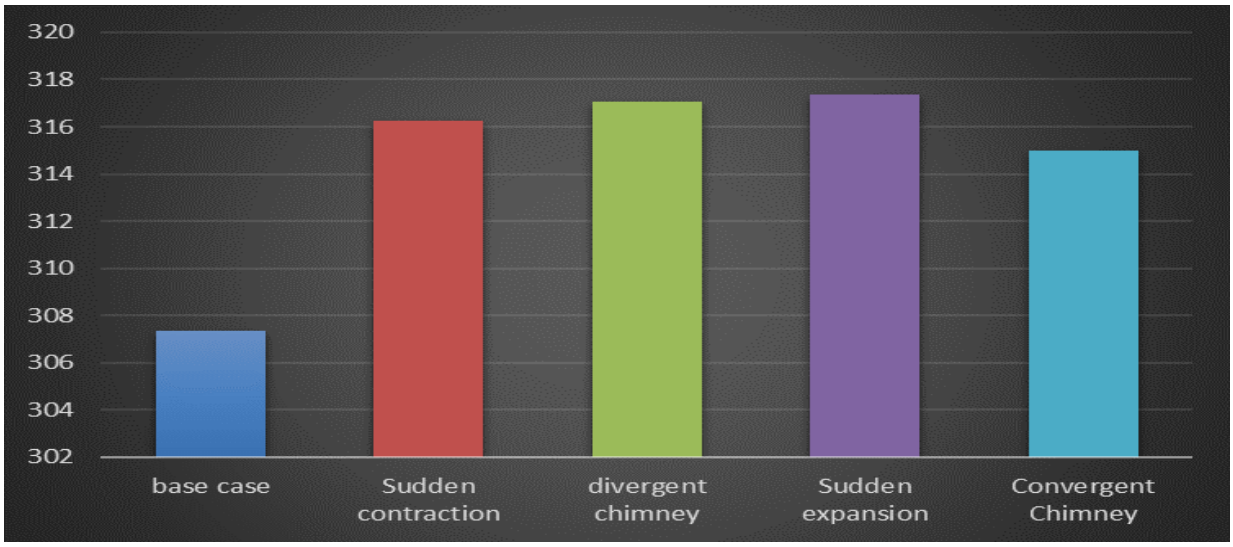

Figure 18: CB Temperature of different chimney(K)

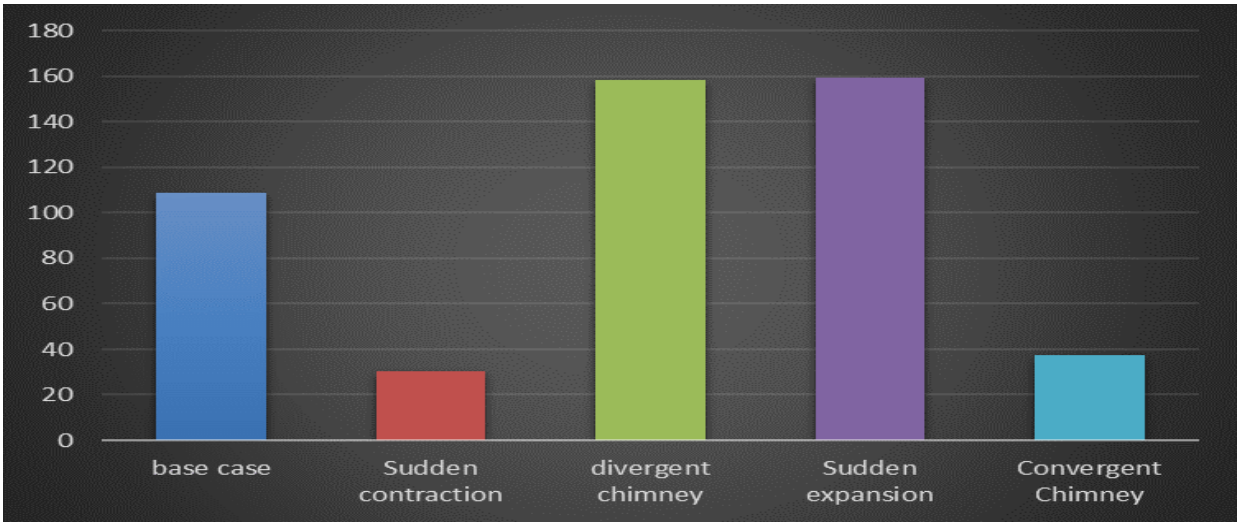

Figure 19: CB Pressure of different chimney (Pascals)

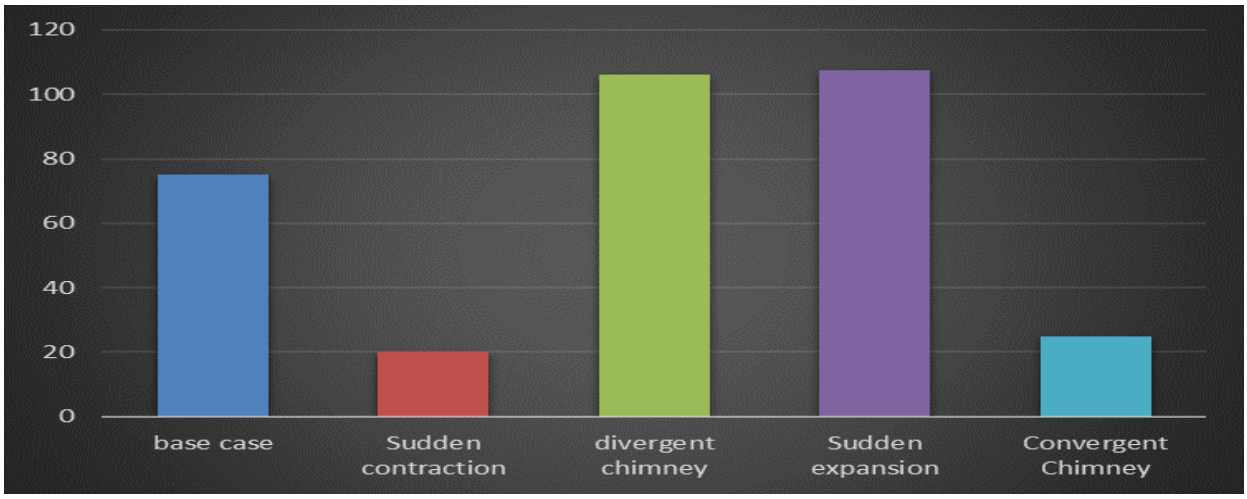

Figure 20: Pressure Drop of different chimney

6. COST ANALYSIS:

Cost analysis of different types chimneys has been calculated. In this comparison outlet diameter of all chimney type has been kept constant at 10 meters. Height of the chimney is taken as 197meter for all type of chimney. In case of sudden expansion two third of the chimney height is taken for lower section whose diameter is taken as 5 meters. In case of sudden contraction two third of the height is taken as 15 meters in diameter and one third of the height is taken as 10 meters. In case of convergent and divergent chimney angle of convergence and divergence are taken as one degree. In case of divergent chimney base diameter is 3.2 meters. In case of convergent chimney base dimeter is 17 meters. Only material cost of aluminium chimney of thickness 0.00125m has been taken for cost comparison. Figure 21 gives the cost and power output of five types of chimneys considered. From the Figure 21 it is evident that sudden expansion types of chimneys costing lowest amongst others and giving lowest cost per unit kilowatt of power output. However, ease of construction and maintenance of the chimney will have to be considered for building any type of solar chimney power plant.

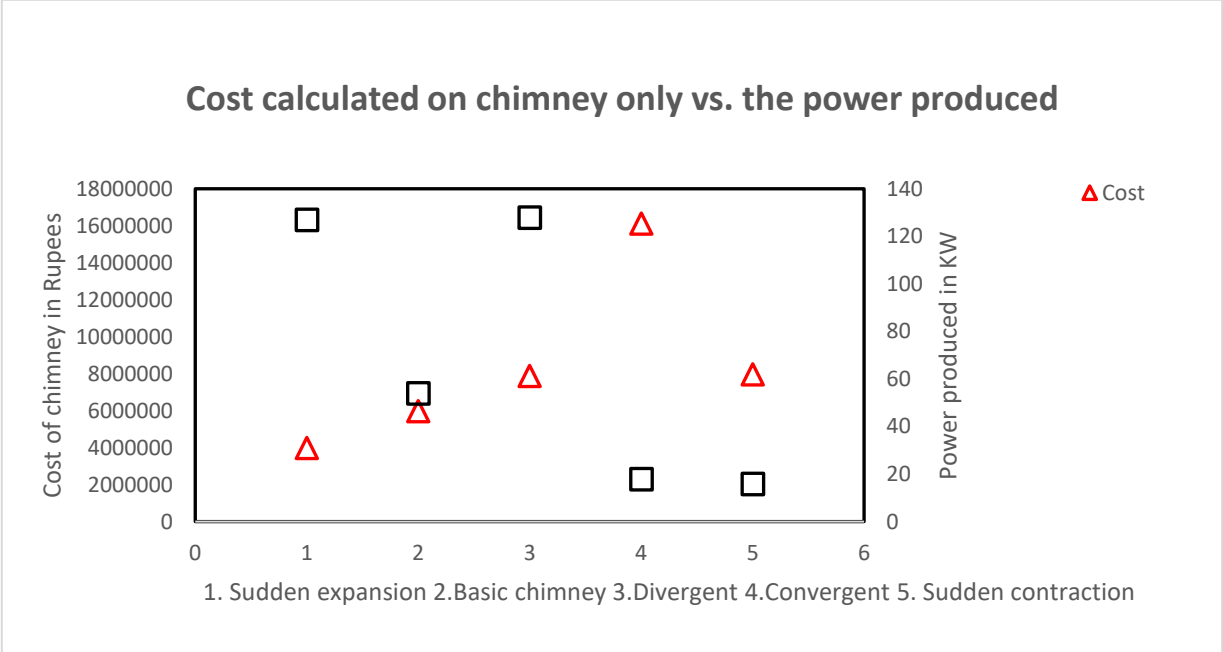

Figure 21: Cost and power output of different types of chimneys

7. CONCLUSION:

The present study analyses three-dimensional thermofluidic flow dynamics and the comparison between convergent, divergent, sudden contraction and sudden expansion type of Chimney for optimizing the performance of a solar chimney power plant (SCPP). The outcome of the study is summarized as follows: Power output of divergent and sudden expansion chimneys are found to be higher than others. Sudden expansion type of chimneys is effective in reducing exit velocities significantly. The sudden increase in flow area converts kinetic energy into pressure energy, increasing static pressure at the chimney exit. Collector efficiency of convergent and sudden contraction are higher than others. It is obvious that there is velocity reduction and retention time for air is more. Overall efficiency of divergent and sudden expansion type of chimney are higher than others. Maximum velocity of divergent and sudden expansion is higher than others. By gradually widening or having sudden expansions, these chimney designs can reduce the pressure losses that occur due to fluid friction. Maximum temperature of sudden expansion and divergent chimneys are higher than others. The sudden expansion chimney design allows for efficient mixing of the incoming air with the hot air collected in the solar collector. As the hot air expands and exits the collector, it rapidly mixes with the incoming cooler air, leading to an increase in temperature. CB velocity of sudden expansion and divergent type of chimneys are higher than others. A sudden expansion chimney design allows the air to rapidly expand as it exits the collector and enters the chimney. This expansion leads to an increase in velocity. CB temperature of sudden expansion and divergent chimneys are higher than others. The sudden expansion chimney design allows for efficient mixing of the incoming air with the hot air collected in the solar collector. As the hot air expands and exits the collector, it rapidly mixes with the incoming cooler air, leading to an increase in temperature. CB pressure of sudden expansion and divergent chimneys are higher than others. Pressure drop of sudden expansion and divergent chimneys are higher than others. The pressure drop in the sudden expansion chimney is more pronounced due to the abrupt increase in cross-sectional area.

Cost analysis of different types chimneys has been calculated. It has been found that sudden expansion type of chimney cost is the lowest amongst others and on the other hand it is also giving highest power output. Cost of power output per unit kilowatt for sudden expansion type of chimney is Rs 31417 compared to divergent type of chimney costing Rs. 61617 which is almost double that of sudden expansion type of chimney, Figure 21.

Sudden expansion can potentially help increase the speed of the updraft, leading to higher energy conversion. Material requirement for a sudden expansion type of chimney is less that a divergent type of chimney. So, Cost per unit power output is less for sudden expansion type of chimney. However, it's essential to balance the design to avoid excessive turbulence or pressure drops that could reduce efficiency. A sudden expansion type of chimney may be advantageous from the point of view of increased air, reduced flow resistance and enhanced mixing but on the other hand an improper design could lead to unintended consequences such as flow separation, turbulence, or reduced updraft velocity. A sudden expansion type of chimney involves engineering challenges in terms of structural integrity, materials, and construction methods to accommodate the change in chimney diameter. The actual gains of such type of chimney might vary depending on factors such as local climate conditions, collector design, and turbine efficiency. The cost of design, construction and maintenance of sudden expansion type of chimney may be higher than a basic type of chimney which could be concluded only after proper analysis. It's essential to conduct through simulations, modeling, and testing to ensure that the sudden expansion will indeed lead to improved performance and justify the additional costs and complexity.

8. ACKNOWLEDGEMENT:
Authors are grateful to the Vice Chancellor of The Assam Kaziranga University, Jorhat Assam, India for giving permission to carry out the research work.

REFERENCES:

1. Haaf W. Solar chimneys part ii: Preliminary test results from the Manzanares pilot plant. Int J Solar Energy 1984;2(2):141–61.https://doi.org/10.1080/01425918408909921
2. Haaf W, Friedrich K, Mayr G, Schlaich J. Solar chimney's part I: principle and construction of the pilot plant in Manzanares. Int J Solar Energy 1983;2(1):3–20.https://doi.org/10.1080/01425918308909911
3. Pasumarthi, N., and S. A. Sherif. "Experimental and theoretical performance of a demonstration solar chimney model—Part I: mathematical model development." International Journal of Energy Research 22.3 (1998): 277-288. https://doi.org/10.1002/(SICI)1099-114X(19980310)22:3<277::AID-ER380>3.0.CO;2-R
4. Pasumarthi, N., & Sherif, S. A. (1998). Experimental and theoretical performance of a demonstration solar chimney model—Part II: experimental and theoretical results and economic analysis. International journal of energy research, 22(5), 443-461. https://doi.org/10.1002/(SICI)1099-114X(199804)22:5<443::AID-ER381>3.0.CO;2-V
5. Lodhi MAK. Application of helio-aero-gravity concept in producing energy and suppressing pollution. Energy Conversion and Management 1999;40:407e21.https://doi.org/10.1016/S0196-8904(98)00104-6
6. Bernardes, M.A., Dos, S., Valle, R.M., and Cortez, M.F., Thermal and technical analyses of solar Chimneys. Int. J. Therm. Sci., 1999, no. 38, pp. 42–50.https://doi.org/10.1016/j.solener.2003.09.012
7. Backstrom, T.W. and Gannon, A.J., Compressible flow through solar power plant chimneys. J. Solar Energy Eng., 2000, no. 122, pp. 138–145.https://doi.org/10.1115/1.1313528
8. Gannon, A.J. and Backstrom, T.W., Solar chimney cycle analysis with system loss and solar collector performance. J. Solar Energy Eng., 2000, no. 122, pp. 133–137.https://doi.org/10.1115/1.1314379
9. Gannon, A.J. and Von Backstrom, T.W., Controlling and Maximizing Solar Chimney Power Output, Proc.1st Int. Conf. on Heat Transfer, Fluid Mechanics and Thermodynamics, Skukuza, 2002.https://doi.org/10.1016/j.solener.2003.08.009
10. Gannon, A.J. and Von Backstrom, T.W., Solar chimney turbine performance. J. Solar Energy Eng., 2003, no. 125, pp. 101–106.https://doi.org/10.1115/1.1530195
11. Pastohr, H., Kornadt, O., and Gurlebeck, K., Numerical and analytical calculation of the temperature and flow field in the upwind power plant. Int. J. Energy Res., 2004, no. 28, pp. 495–510.https://doi.org/10.1002/er.978
12. Schlaich, J., Bergermann, R., Schiel, W., and Wein rebe, G., Design and commercial solar updraft tower systems- Utilization of solar induced convective flows for power generation. J. Solar Energy Eng., 2005, no. 127, pp. 117–124.https://doi.org/10.1115/1.1823493
13. Pretorius, J.P. and Kroger, D.G., Solar chimney power plant performance. J. Solar Energy, 2006, vol. 128, no. 3, pp. 302–311.https://doi.org/10.1115/1.2210491
14. Bilgen, E. and Rheault, J., Solar chimney power plants for high latitudes. Solar Energy, 2006, no. 79, pp. 449–458.https://doi.org/10.1016/j.solener.2005.01.003

15. Koonsrisuk, A. and Chitsomboon, T., Dynamic similarity in solar chimney modeling. Solar Energy, 2007, no. 81, pp. 1439–1446.https://doi.org/10.1016/j.solener.2007.03.003
16. Cuce, Erdem; Saxena, Abhishek; Cuce, Pinar Mert; Sen, Harun; Guo, Shaopeng; Sudhakar, K. Performance assessment of Solar Chimney Power Plants with the impact of divergent and convergent chimney geometry. International Journal of Low-Carbon Technology (2021), 16(3), 704-714.https://doi.org/10.1093/ijlct/ctaa097
17. Siyang Hu, Dennis Y.C. Leung, John C.Y. Chan, Impact of the geometry of divergent chimneys on the power output of a Solar Chimney Power Plant. Energy, Vol. 120, 1 February 2017, Pages 1-11.https://doi.org/10.1016/j.energy.2016.12.098
18. Das, Pritam; V.P., Chandramohan, Performance characteristics of divergent chimney solar updraft tower plant. International Journal of Energy Research (2021), 45(12), 17159-17174.https://doi.org/10.1002/er.5304
19. Alit Koonsrisuk, Tawit Chitsomboon, Effects of flow area changes on the potential of solar chimney power plants. Energy, Vol. 51, 1 March 2013, pages 400-406.https://doi.org/10.1016/j.energy.2012.12.051
20. Abdallah Bouabidi, Ahmed Ayadi, Haytham Nasraoui, Zied Driss, Mohamed Salah Abid, Study of solar chimney in Tunisia: Effect of the chimney configuration on the local flow characteristics. Energy and Buildings, Vol. 169, 15 June 2018, Pages 27-38.https://doi.org/10.1016/j.enbuild.2018.01.049
21. Ajeet Pratap Singh, Amit Kumar, Akshay Veer, O.P. Singh, A Novel concept of integrating bell-mouth inlet-in converging-diverging solar chimney power plant. Renewable Energy, Vol. 169, May 2021, pages 318-334.https://doi.org/10.1016/j.renene.2020.12.120
22. Lal S, Kaushik SC, Hans R. Experimental investigation and CFD simulation studies of a laboratory scale Solar chimney for power generation. Sustain Energy Technol Assess 2016;13:13–22.https://doi.org/10.1016/j.seta.2015.11.005
23. Guo P, Li T, Xu B, Xu X, Li J. Questions and current understanding about solar chimney power plant: A review. Energy Convers Manage 2019;182:21–33. https://doi.org/10.1016/j.enconman.2018.12.063
24. Hanna MB, Mekhail TA-M, Dahab OM, Esmail MFC, Abdel-Rahman AR. Experimental and numerical investigation of the Solar chimney power plant's turbine. Open J Fluid Dyn 2016;6:332–42.https://doi.org/10.4236/ojfd.2016.64025
25. Maghrebi MJ, Nejad RM, Masoudi S. Performance analysis of sloped Solar chimney power plants in the southwestern region of Iran. Int J Ambient Energy 2017;38(Issue-6):542–9. https://doi.org/10.1080/01430750.2016.1155487
26. Bouabidi A, Nasraoui H, Ayadi A, Driss Z, Abid MS, 2019, Numerical analysis of chimney diameter effect on the fluid flow and the heat transfer characteristics within the solar tower, 41, Issue-20, Energy Sources, Part A: Recovery, Utilization, and Environmental Effects. https://doi.org/10.1080/15567036.2019.15686311
27. Nasraoui H, Driss Z, Ayedi A, Kchaou H. Numerical and experimental study of the aerothermal characteristics in solar chimney power plant with hyperbolic chimney shape. Arabian J Sci Eng 2019;44(Issue-9):7491–504. https://doi.org/10.1007/s13369-019-03821-x
28. Chikere AO, Al-Kayiem HH, Karim ZAA. Review the enhancement techniques and introduction of an alternate enhancement technique for solar chimney power plant. J Appl Sci 2011;11:1877–84. https://doi.org/10.3923/jas.2011.1877.1884

29. Cao F, Zhao L, Li H, Guo L. Performance analysis of conventional and sloped Solar chimney power plants in China. Appl Therm Eng 2013;50(Issue-1):582–92. https://doi.org/10.1016/j.applthermaleng.2012.06.038
30. Sangi R. Performance evaluation of solar chimney power plants in Iran. Renew Sustain Energy Rev 2012;16(1):704–10. https://doi.org/10.1016/j.rser.2011.08.035
31. Gholamalizadeh E, Kim M-H. CFD (computational fluid dynamics) analysis of a solar-chimney power plant with an inclined collector roof. Energy 2016;107:661–7. https://doi.org/10.3390/en9110971
32. I. Dincer, Heat Transfer in Food Cooling Applications, Taylor & Francis, Washington, DC. (1997); and C. Borgnakke and R.E. Sonntag, Thermodynamic and Transport Properties, Wiley, New York (1997).Appendix B: Thermophysical Properties - Thermal Energy Storage - Wiley Online Library https://onlinelibrary.wiley.com/doi/pdf/10.1002/9780470970751.app2.
33. N. Biswas, D.K.Mandal, N.K.Manna, A.C.Benim, Novel stair-shaped ground absorber for performance enhancement of solar chimney power plant: a numerical study 120466(2023). https://doi.org/10.1016/j.applthermaleng.2023.12046
34. A. Koonsrisuk, T. Chitsomboon, Mathematical modeling of solar chimney power plants, Energy 51 (2013) 314–322. https://doi.org/10.1016/j.energy.2012.10.038
35. P. Guo, J. Li, Y. Wang, Numerical simulations of solar chimney power plant with radiation model, Rene. Energy 62 (2014) 24–30. https://doi.org/10.1016/j.renene.2013.06.039
36. S.R. Keshari, V.P. Chandramohan, P. Das, A 3D numerical study to evaluate optimum collector inclination angle of Manzanares solar updraft tower power plant, Sol. Energy 226 (2021) 455–467.https://doi.org/10.1016/j.solener.2021.08.062
37. R. Sangi, M. Amidpour, B. Hosseinizadeh, Modeling and numerical simulation of solar chimney power plants, Sol. Energy 85 (2011) 829–838. https://doi.org/10.1016/j.solener.2011.01.011
38. A. Kasaeian, M. Ghalamchi, M. Ghalamchi, Simulation and optimization of geometric parameters of a solar chimney in Tehran, Energy Conv. Manage. 83(2014) 28–34. https://doi.org/10.1016/j.enconman.2014.03.042
39. E. Cuce, P.M. Cuce, H. Sen, K. Sudhakar, U. Berardi, U. Serencam, Impacts of ground slope on main performance figures of solar chimney power plants: a comprehensive CFD research with experimental validation, Int. J. Photoenergy 6612222 (2021) 1–11. https://doi.org/10.1155/2021/6612222